Phenomenology of scalar and vector mesons in the linear σ model

Pyungwon Ko*
Department of Physics, Hong-Ik University, Seoul 121-791, Korea

Serge Rudaz†
School of Physics and Astronomy, University of Minnesota, Minneapolis, Minnesota 55455
(Received 22 February 1994)

A generalization of the linear σ model that includes vector and axial vector mesons is presented. The resulting effective Lagrangian incorporates some new features not previously considered. The consistency of the model is successfully checked by applying it to a variety of processes, including low-energy $\pi\pi$ scattering and a_1 decays. An interesting feature of this new effective Lagrangian is that it provides a natural mechanism leading to a reduction of the $\sigma \to \pi\pi$ decay width relative to the expected value in the original linear σ model. The generalization of the Wess-Zumino effective action appropriate to the linear σ model is also considered.

PACS number(s): 12.39.Fe, 11.30.Rd, 12.40.Vv, 14.40.Cs

I. INTRODUCTION

The linear $SU(2)_L \times SU(2)_R$ σ model, including the pion and its isoscalar, scalar chiral partner the σ meson, provides a nice, explicit field theoretic realization of the idea of broken chiral symmetry and gives a reasonable quantitative description of the low energy interactions of pions. However, the difficulty of identifying the σ with any one of the many scalar states found in the Particle Data Group (PDG) compilation [1] (certainly, one finds too many states below 2 GeV to fill just one $^3P_0$ $\bar{q}q$ nonet) has led to a relative neglect of this model as a serious basis for phenomenology. The difficulty here is to be traced directly to the expression for the $\sigma \to \pi\pi$ width, which is given by (including the pion mass as an explicit chiral symmetry breaking effect)

$$\Gamma(\sigma \to \pi\pi) = \frac{3m_\sigma^3}{32\pi f_\pi^2}\left(1-\frac{m_\pi^2}{m_\sigma^2}\right)^2\left(1-\frac{4m_\pi^2}{m_\sigma^2}\right)^{1/2}. \tag{1.1}$$

This is unphysically large: with $f_\pi = 93$ MeV, one sees that the width of the σ equals its mass at $m_\sigma \simeq 600$ MeV, and rises quickly thereafter. This is apparently inconsistent with even the large width (500 – 600 MeV) of the broad scalar isoscalar state around 1 GeV that is responsible for the I=0, S-wave $\pi\pi$ interaction [2], which is the clear candidate for the σ meson, and which appears in the 1994 PDG table [1] as the $f_0(1300)$.

The purpose of this paper is to extend the $SU(2)_L \times SU(2)_R$ linear σ model to include the vector mesons ρ and a_1 as chiral partners, including new elements not present in previous work found in the old literature. As an important consequence, we will find that the inclusion of vector and axial vector mesons in a chirally invariant way can lead to a drastic reduction of the $\pi\pi$ decay width of σ, alleviating the difficulty mentioned above.

Our aim is to provide a consistent phenomenological picture of the known properties of the vector mesons ρ and a_1 as well: for this purpose, the linear σ model must be extended to include nonrenormalizable higher dimension terms, as will be detailed below.

The plan of the paper is as follows: in Sec. II A, vector and axial vector mesons (ρ and a_1) are introduced in the linear σ model as gauge fields associated with the *local* $SU(2)_L \times SU(2)_R$ chiral symmetry. This local chiral symmetry is broken to the global symmetry by mass terms for ρ and a_1. In our model, vector and axial vector mesons get massive through both the bare mass and spontaneous chiral symmetry breaking [see Eqs. (2.20) and (2.21)]. This feature is a new one compared to the conventional approaches, where $m_\rho = m_{a_1} = m_0$ in the phase of unbroken chiral symmetry, and this degeneracy is broken by $f_\pi \neq 0$ and π-a_1 mixing. We consider two dimension-6 operators in addition to the original gauged linear σ model in order to get better overall consequences for ρ and a_1 phenomenology. In Sec. II B, the electromagnetic field is introduced in a way consistent with vector dominance hypothesis and $U(1)_{em}$ gauge invariance. In Sec. II C, our model is compared with previous ones, with emphasis on the study of deviations from the usually made assumptions such as complete vector dominance, saturations of Weinberg's sum rules using single pole approximations and Kawarabayashi-Suzuki-Fayyazuddin-Riazuddin (KSFR) relation. In Secs. III A and III B, we discuss the $\pi\pi$ and the decay width of σ in our model, with special attention to show how the low energy theorem for $\pi\pi$ scattering remains intact even in the presence of vector and axial vector mesons. We also

*Electronic address: pko@phyb.snu.ac.kr
†Electronic address: rudaz@mnhep.hep.umn.edu

find the σ width can be substantially smaller than in the case of the original linear σ model, because of π-a_1 mixing. In Sec. IV A, the decay modes $a_1 \to \rho\pi$ and $a_1^\pm \to \pi^\pm\gamma$ are described. Our model reproduces the result of current algebra and PCAC (partial conservation of axial vector current) on $a_1 \to \rho\pi$. In Sec. IV B, we consider $a_1^\pm \to \pi^\pm\gamma$ in our framework and compare with other theoretical predictions as well as the data. In Sec. IV C, it is found that the non-$\rho\pi$ contributions to $a_1 \to 3\pi$ can be vanishingly small. Generalization of the Wess-Zumino anomaly in the linear σ model is given in Sec. V. Our predictions on various processes are summarized in Sec. VI. Interaction Lagrangians relevant to processes considered in this work are collected in Appendix A. Appendix B contains explicit expressions for $a_1 \to 3\pi$ discussed in Sec. IV C.

II. THE σ MODEL WITH VECTOR AND AXIAL VECTOR MESONS

A. Model Lagrangians

The linear σ model [3] has the following particle content: isotriplet pseudoscalars (π^a) and the isosinglet scalar (σ). They form a $(\frac{1}{2},\frac{1}{2})$ representation of $SU(2)_L \times SU(2)_R$, and are grouped into

$$\Sigma = \sigma + i\boldsymbol{\tau}\cdot\boldsymbol{\pi}, \tag{2.1}$$

which transforms under $SU(2)_L \times SU(2)_R$ as

$$\Sigma \longrightarrow L\Sigma R^\dagger. \tag{2.2}$$

$\boldsymbol{\tau}$'s are the Pauli spin matrices, and $\mathbf{t} \equiv \boldsymbol{\tau}/2$ are generators of the SU(2) Lie algebra.

The Gell-Mann–Levy linear σ model [3] is defined by the Lagrangian density

$$\mathcal{L}_0 = \frac{1}{4}\ \mathrm{Tr}\ \left[\partial_\mu\Sigma\ \partial^\mu\Sigma^\dagger\right] - \frac{\lambda}{8}\ \mathrm{Tr}\ \left[\left(\Sigma\Sigma^\dagger - f_0^2\right)^2\right]. \tag{2.3}$$

$\mathcal{L}_0$ is invariant under global $SU(2)_L \times SU(2)_R$ transformations, which leads to the conserved Noether currents:

$$\mathbf{V}_\mu = \boldsymbol{\pi} \times \partial_\mu\boldsymbol{\pi}, \tag{2.4}$$

$$\mathbf{A}_\mu = \sigma\ \partial_\mu\boldsymbol{\pi} - \boldsymbol{\pi}\partial_\mu\sigma. \tag{2.5}$$

The pion mass is introduced through a symmetry-breaking potential, which can be chosen in the convenient form

$$\mathcal{L}_{\mathrm{SB}} = -\frac{\mu_\pi^2}{2}\ \left[\boldsymbol{\pi}^2 + (\sigma - f_0)^2\right], \tag{2.6}$$

which yields the usual form of PCAC:

$$\partial_\mu\mathbf{A}^\mu = m_\pi^2 f_\pi \boldsymbol{\pi}. \tag{2.7}$$

[We have used $f_0 = f_\pi$ and $\mu_\pi = m_\pi$ in Eq. (2.7).]

Now, we add isotriplet vector and axial vector mesons ($\boldsymbol{\rho}$ and $\mathbf{a}_1$) to the linear σ model in a way consistent with the current-field identity and vector meson dominance hypothesis. This can be achieved by regarding $\boldsymbol{\rho}$ and $\mathbf{a}_1$ as phenomenological gauge fields associated with a *local* chiral $SU(2)_L \times SU(2)_R$. Since the chiral symmetry in QCD is a global symmetry, this local chiral symmetry has to be broken, for example, by adding mass terms for vector and axial vector mesons. A mass term yields the correct form of the field-current identity when we construct vector and axial vector currents using the Noether method [4,5].

Let us introduce left and right gauge fields,

$$l_\mu \equiv \boldsymbol{l}_\mu\cdot\mathbf{t} = \left(\boldsymbol{\rho}_\mu + \mathbf{a}_\mu\right)\cdot\mathbf{t}, \tag{2.8}$$

$$r_\mu \equiv \mathbf{r}_\mu\cdot\mathbf{t} = \left(\boldsymbol{\rho}_\mu - \mathbf{a}_\mu\right)\cdot\mathbf{t}, \tag{2.9}$$

which form adjoint representations of $SU(2)_L$ and $SU(2)_R$, respectively. The field strength tensors for l_μ and r_μ are defined as usual:

$$l_{\mu\nu} \equiv \boldsymbol{l}_{\mu\nu}\cdot\mathbf{t} = \partial_\mu l_\nu - \partial_\nu l_\mu - ig\ [l_\mu, l_\nu],$$

or

$$\boldsymbol{l}_{\mu\nu} = \partial_\mu\boldsymbol{l}_\nu - \partial_\nu\boldsymbol{l}_\mu + g\ \boldsymbol{l}_\mu\times\boldsymbol{l}_\nu,$$

and similarly for $r_{\mu\nu}$. We will use both types of notation interchangeably in the following. The kinetic energy term for these gauge fields are given by the usual Maxwell term

$$\mathcal{L}_{\mathrm{kin}}(l,r) = -\frac{1}{4}\ \mathrm{Tr}\ \left[l_{\mu\nu}l^{\mu\nu} + r_{\mu\nu}r^{\mu\nu}\right]. \tag{2.10}$$

Parity is conserved since we symmetrize our Lagrangian under $L \leftrightarrow R$.

To break the hypothetical *local* chiral symmetry into the *global* chiral symmetry and make the vector and the axial vector mesons massive, we add the mass-like terms

$$\mathcal{L}_m = \tfrac{1}{2}\ m_0^2\ \mathrm{Tr}\left[l_\mu l^\mu + r_\mu r^\mu\right] + \tfrac{1}{4}\ bg^2\ \mathrm{Tr}[\Sigma\Sigma^\dagger]$$
$$\times\mathrm{Tr}\left[\ l_\mu l^\mu + r_\mu r^\mu\ \right] - cg^2\ \mathrm{Tr}\left[\ l^\mu\Sigma r_\mu\Sigma^\dagger\ \right]. \tag{2.11}$$

In earlier work using phenomenological massive Yang-Mills gauge fields, only the m_0^2 term was kept in $\mathcal{L}_m$, which generates equal masses for ρ and a_1 before chiral symmetry breaking. (This degeneracy is lifted by spontaneous chiral symmetry breaking: this is the Higgs mechanism.) For $b = c = 0$, we recover the usual current-field identities [4,5].

The new b, c terms give additional contributions to the Noether currents and current-field identities. After chiral symmetry breaking, these terms generate additional contributions to the masses of vector and axial vector mesons, and play an important role in describing the process $a_1 \to \sigma\pi$. [The b term was first considered in the linear σ model with ω meson to study nuclear matter saturation [6]. The c term was first introduced in Ref. [7] in the nonlinear σ model with vector and axial vector mesons in order to get the correct $\rho \to \pi\pi$ width when one eliminates the a_1 meson. However, the effects of the c term on m_{a_1} and the KSFR relation were not studied in detail.] For example, one can imagine setting $m_0^2 = 0$, since the b, c terms can provide the vector and the axial

vector with their masses after spontaneous chiral symmetry breaking, $\langle\sigma\rangle \equiv f_0 \neq 0$.

Except for $\mathcal{L}_m$, the couplings of $\boldsymbol{\rho}$ and $\mathbf{a}$ to other matter fields are assumed to be consistent with the gauge principle. The ordinary derivative in Eq. (2.3) is replaced by the covariant derivative

$$D_\mu\Sigma = \partial_\mu\Sigma - igl_\mu\Sigma + ig\Sigma r_\mu. \tag{2.12}$$

Using this covariant derivative, one can generalize Eq. (2.3) into

$$\mathcal{L}_0^{\rm new} = \frac{1}{4}\ {\rm Tr}\ \left[D_\mu\Sigma\ D^\mu\Sigma^\dagger\right] - \frac{\lambda}{8}\ {\rm Tr}\ \left[(\Sigma\Sigma^\dagger - f_0^2)^2\right] + \mathcal{L}_{\rm kin}(l,r) + \mathcal{L}_m. \tag{2.13}$$

This Lagrangian with $b = c = 0$ and $\mathcal{L}_{SB}$ (2.6) was essentially known by the late sixties [5], and reproduces the results based on current algebra and PCAC obtained then. As we shall shortly see, the systematics of ρ decay require the inclusion of an additional term, however.

We note that the Noether currents of this effective Lagrangian (2.13) are consistent with the current-field identities

$$\mathbf{V}_\mu^{\rm new} = \frac{1}{g}\ \left[m_0^2 + bg^2\ (\sigma^2+\boldsymbol{\pi}^2) - cg^2\sigma^2\right]\ \boldsymbol{\rho}_\mu - cg\ \left[2\sigma\boldsymbol{\pi}\times\mathbf{a}_\mu + (\boldsymbol{\rho}_\mu\cdot\boldsymbol{\pi}\boldsymbol{\pi} - \boldsymbol{\pi}\times(\boldsymbol{\rho}_\mu\times\boldsymbol{\pi}))\right], \tag{2.14}$$

$$\mathbf{A}_\mu^{\rm new} = \frac{1}{g}\ \left[m_0^2 + bg^2\ (\sigma^2+\boldsymbol{\pi}^2) + cg^2\sigma^2\right]\ \mathbf{a}_\mu + cg\ \left[2\sigma\boldsymbol{\pi}\times\boldsymbol{\rho}_\mu + (\mathbf{a}_\mu\cdot\boldsymbol{\pi}\boldsymbol{\pi} - \boldsymbol{\pi}\times(\mathbf{a}_\mu\times\boldsymbol{\pi}))\right]. \tag{2.15}$$

In order to understand the dynamics of $\boldsymbol{\pi}, \sigma, \boldsymbol{\rho}$, and $\mathbf{a}_1$, using this gauged linear σ model, it is necessary to express the Lagrangian in terms of physical fields. The ground state can be chosen as $\langle\sigma\rangle = f_0, \langle\boldsymbol{\pi}\rangle = 0$. This spontaneous symmetry breaking induces a mixing between $\boldsymbol{\pi}$ and $\mathbf{a}_1$. Therefore, we have to make field redefinitions[1]

$$\sigma \to \sigma + f_0, \tag{2.16}$$

$$\mathbf{a}_\mu \to \mathbf{a}_\mu + hD_\mu\boldsymbol{\pi}, \tag{2.17}$$

and choose the parameter h in such a way that there is no mixing between $\boldsymbol{\pi}$ and $\mathbf{a}$ fields. Finally, we need to do a wave function renormalization for $\boldsymbol{\pi}$ to get the canonical form of the kinetic energy term for the renormalized pion fields $(\boldsymbol{\pi}_r)$: $\boldsymbol{\pi} = \boldsymbol{\pi}_r/\sqrt{Z_\pi}$. After this procedure, detailed in Appendix A, we get the relations

$$m_\pi^2 = \frac{\mu_\pi^2}{Z_\pi}, \tag{2.18}$$

$$m_\sigma^2 = 2\lambda f_0^2 + \mu_\pi^2 = 2\lambda\frac{f_\pi^2}{Z_\pi} + m_\pi^2 Z_\pi, \tag{2.19}$$

$$m_\rho^2 = m_0^2 + (b-c)\ g^2 f_0^2, \tag{2.20}$$

$$m_{a_1}^2 = m_0^2 + (b+c+1)\ g^2 f_0^2, \tag{2.21}$$

$$h = \frac{gf_0}{m_0^2 + (b+c+1)\ g^2 f_0^2} = \frac{gf_0}{m_{a_1}^2}, \tag{2.22}$$

$$Z_\pi = 1 - \frac{g^2 f_0^2}{m_{a_1}^2} = 1 - \left(\frac{1}{2c+1}\right)\left(1 - \frac{m_\rho^2}{m_{a_1}^2}\right). \tag{2.23}$$

Defining $a \equiv m_{a_1}^2/m_\rho^2$ and $f_\pi \equiv f_0\sqrt{Z_\pi} = 93$ MeV, we get

$$m_{a_1}^2 - m_\rho^2 = (a-1)\ m_\rho^2 = \frac{(2c+1)}{Z_\pi}\ g^2 f_\pi^2, \tag{2.24}$$

so that

$$m_\rho^2 = \frac{g^2 f_\pi^2}{aZ_\pi(1-Z_\pi)}. \tag{2.25}$$

This would be nothing but the KSFR relation [8], were we to choose $a = 2$ (for which $m_{a_1} = \sqrt{2}\ m_\rho = 1090$ MeV), $Z_\pi = 1/2$, and $g_{\rho\pi\pi} = g$.

However, the $\rho\pi\pi$ coupling following from (2.13) has a strong momentum dependence because of the $\pi - a_1$ mixing, as given by Eq. (A12) with $\kappa_6 = \zeta_6 = 0$. The corresponding $\rho\pi\pi$ vertex is

$$F_{\rho\pi\pi}^{(0)}(q^2) = \frac{gm_\rho^2}{Z_\pi m_{a_1}^2}\ \left[1 - \frac{g^2 f_\pi^2}{2Z_\pi m_{a_1}^2}\ \frac{q^2}{m_\rho^2}\right], \tag{2.26}$$

so that

$$g_{\rho\pi\pi} \equiv F_{\rho\pi\pi}^{(0)}(m_\rho^2) = \frac{g}{2}\ [1+Z_\pi]. \tag{2.27}$$

If we fix $g = 5.04$ from $\rho^0 \to e^+e^-$ [2] and solve (2.23) and $g_{\rho\pi\pi} \equiv F_{\rho\pi\pi}^{(0)}(m_\rho^2)$, we get $Z_\pi = 0.33$, and $m_{a_1} = 1.0$ GeV which is too small. On the other hand, if we fix $m_{a_1} = 1.26$ GeV and solve (2.23) and $g_{\rho\pi\pi} \equiv F_{\rho\pi\pi}^{(0)}(m_\rho^2)$, we get $Z_\pi = 0.20, g = 5.40$, and $c = -0.11$. Thus, we get $\Gamma(\rho^0 \to e^+e^-) = 7.77$ keV, which is 15% larger than the measured value, (6.77 ± 0.32) keV. Assuming this be tolerable and studying a_1 decays, one gets too small a decay rate for $a_1 \to \rho\pi$,

$$\Gamma(a_1 \to \rho\pi) \approx 88\ {\rm MeV},$$

regardless of m_0. So, we always end up with wrong phenomenology with the above form of gauged linear σ model with dimension ≤ 4. To cure this problem, we add a dimension-6 operator[3]

---

[1] One could make a shift, $\mathbf{a}_\mu \to \mathbf{a}_\mu + h\partial_\mu\boldsymbol{\pi}$, instead. When coupled with electromagnetic field, however, this shift yields a wrong seagull term. See the next subsection for details.

[2] The introduction of electromagnetic interactions is dealt with in the next subsection.

[3] This term is essentially the same, in the language of effective Lagrangians, as the δ term introduced by Schnitzer and Weinberg [9]. It is nothing but the κ term in Ref. [5].

$$-\frac{i\kappa_6 g}{4m_\rho^2}\ \mathrm{Tr}\ \left[l_{\mu\nu}\ D^\mu\Sigma D^\nu\Sigma^\dagger + r_{\mu\nu}\ D^\mu\Sigma^\dagger D^\nu\Sigma\right]. \quad (2.28)$$

Then, the $\rho\pi\pi$ vertex is modified into

$$F_{\rho\pi\pi}(q^2) = \frac{gm_\rho^2}{Z_\pi m_{a_1}^2}\ \left[1 - \frac{g^2 f_\pi^2}{2Z_\pi m_{a_1}^2}\ \frac{q^2}{m_\rho^2}\right] - \frac{1}{2}\ g\kappa_6 Z_\pi\ \frac{q^2}{m_\rho^2}. \quad (2.29)$$

One can fix κ_6 demanding

$$g_{\rho\pi\pi} \equiv F_{\rho\pi\pi}(m_\rho^2) = \frac{gm_\rho^2}{Z_\pi m_{a_1}^2}\ \left[1 - \frac{g^2 f_\pi^2}{2Z_\pi m_{a_1}^2}\right] - \frac{1}{2}\ g\kappa_6 Z_\pi = 6.05 \quad (2.30)$$

to give the correct width for $\rho \to \pi\pi$. This will also fix the problem of a small decay rate for $a_1 \to \rho\pi$, as discussed in Sec. IV A.

From (2.29), one can write the expression

$$gg_{\rho\pi\pi}(m_\rho^2) = \frac{m_\rho^2}{2f_\pi^2}\ \left[(1 - Z_\pi^2) - g^2\kappa_6 Z_\pi \frac{f_\pi^2}{m_\rho^2}\right], \quad (2.31)$$

to be compared with the original form of the KSFR relation

$$gg_{\rho\pi\pi}(m_\rho^2) = \frac{m_\rho^2}{2f_\pi^2} + \cdots, \quad (2.32)$$

where the ellipses means uncalculable or ignored contributions from the Schwinger terms, higher-order terms in pion momenta and the higher resonances, etc. Note that our result (2.31) reduces into (2.32) in the unphysical limit of $Z_\pi \to 0$ and $Z_\pi m_{a_1}^2 \to$ const. In our approach, we can evaluate these corrections to the original form of the KSFR relation by the finite mass of a_1 resonance, and get improved overall phenomenology.

The inclusion of higher dimensional operators in the linear σ model is clearly consistent with the view taken here that it should be seen as an effective theory: while the model, in its original form [3] involving only $\sigma, \boldsymbol{\pi}$, and the nucleon, is perturbatively renormalizable (and in fact, not unexpectedly for a strong-coupling problem, fails if taken seriously in one-loop order [10]), it is clear that this is not a physically limiting consideration. However, in the context of the linear σ-model, operator dimensionality is not an immediately useful organizing criterion, unlike the case of the nonlinear σ model. This is due to the fact that after the field redefinitions (2.16),(2.17), a term in the Lagrangian of any given dimensionality d will in general give rise to a number of terms of dimension d as well as $d \pm 1, d \pm 2$, and so on. [Notice that the field redefinition (2.16) lowers the dimension by one, whereas (2.17) increases the dimension by one.] This is a necessary consequence of the physics of spontaneous symmetry breaking as described by the linear σ model. For example, the dimension 4 operators involving b and c provide a description of which part of the vector meson masses (dimension 2) is due directly to chiral symmetry breaking, while κ_6 contributes in an important way to the $\rho\pi\pi$ vertex which is nominally of dimension 4 and dimension 6. The choice of which operators should be present in the model is dictated by the need for a consistent phenomenology in leading order.

Summarizing, our model Lagrangian consists of (2.13), (2.28), (2.44), and (2.38). [Relevant parts of our model Lagrangian, the vector and the axial vector currents, and symmetry relations analogous to (2.20)–(2.25) are given in the Appendix in case of arbitrary ζ_6 which is defined in Sec. II C.] In the limit of an infinitely heavy σ meson, it reduces into the nonlinear chiral Lagrangian with vector and axial vector mesons considered in Ref. [11], except for the b and c terms. Since these b and c terms have not been considered in the literature, our model Lagrangian leads to different phenomenology of a_1 meson. In the nonlinear limit,

$$\Sigma \to f_0 e^{i\boldsymbol{\pi}\cdot\mathbf{t}/f_0},$$

and the b term is absorbed into the bare mass term making a shift, $m_0^2 \to (m_0^2 + bg^2 f_0^2)$. On the other hand, the c term remains:

$$c\ \mathrm{Tr}[l_\mu \Sigma r^\mu \Sigma^\dagger] \to c f_0^2\ \mathrm{Tr}[l_\mu U r^\mu U^\dagger], \quad (2.33)$$

contrary to previous models. Therefore, even in the absence of σ, our model predictions on $a_1 - \rho - \pi$ system are different from previous models. Especially, one can accomodate a large decay width of $a_1 \to \rho\pi$ even without ζ_6 term. (In Ref. [11], this could not be achieved without the ζ_6 term.)

B. Electromagnetic interactions

To describe electromagnetic processes such as $\rho \to e^+e^-$ and $a_1 \to \pi\gamma$, we need to introduce the electromagnetic field in a gauge invariant way, implementing the idea of CVC (conserved vector current) hypothesis. This was studied in detail by Kroll, Lee, and Zumino [12], and a brief review can be found in Ref. [5].

Let us first note that an $\mathrm{SU}(2)_V$ gauge transformation in the third direction, for the third component of the isovector vector field, looks like a $\mathrm{U}(1)_V$ gauge transformation

$$\delta\rho_\mu^0 = \frac{1}{g}\ \partial_\mu\alpha_3, \quad (2.34)$$

where $\rho_\mu^0 = \rho_{\mu,3}$ and $\boldsymbol{\alpha}$ is the $\mathrm{SU}(2)_V$ gauge-transformation parameter. If we introduce the electromagnetic-gauge field B_μ which transforms as

$$\delta B_\mu = \frac{1}{e}\ \partial_\mu\alpha_3, \quad (2.35)$$

the combination

$$\rho_\mu^0 - \frac{e}{g}\ B_\mu$$

is invariant under Eqs. (2.34) and (2.35). Since the masslike terms are not invariant under Eq. (2.34), we can replace the ρ_μ^0 in the masslike terms by

$$\rho_\mu^0 \longrightarrow \rho_\mu^0 - \frac{e}{g} B_\mu. \tag{2.36}$$

(Other terms with covariant derivatives are invariant by themselves, so they do not change.) We also add the kinetic term for the photon field:

$$\mathcal{L}_{\rm kin}(B) = -\tfrac{1}{4} B_{\mu\nu} B^{\mu\nu}. \tag{2.37}$$

At the one-photon level, we recover

$$\mathcal{L}_{\rm em} = -e V_\mu^3 B^\mu, \tag{2.38}$$

where V_μ is the vector current of our model constructed by the Noether method. At the two-photon level, our prescription gives interactions of hadrons and photons in a $U(1)_{\rm em}$ gauge invariant way. For example, we recover the ordinary seagull term for electromagnetic coupling of charged pions by replacing ρ_μ by $\rho_\mu + eB_\mu/g$. However, this would not be possible, if we had made a shift,

$$\mathbf{a}_\mu \to \mathbf{a}_\mu + h\partial_\mu \boldsymbol{\pi}. \tag{2.39}$$

More specifically, the interaction of charged pions with photon fields would have been given by

$$-eB_\mu(\pi_r^+ \partial^\mu \pi_r^- - \pi_r^- \partial^\mu \pi_r^+) + \frac{e^2}{Z_\pi} B_\mu B^\mu \pi_r^+ \pi_r^-,$$

which is not gauge invariant, unless $Z_\pi = 1$. Thus, we can justify the shift of $\mathbf{a}_\mu$ by $hD_\mu\boldsymbol{\pi}$.

Now, one can consider $\rho^0 \to e^+e^-$. From Eq. (2.38), one can derive

$$\Gamma(\rho^0 \to e^+e^-) = \frac{4\pi\alpha^2}{g^2} \frac{m_\rho}{3}. \tag{2.40}$$

Using $\Gamma(\rho^0 \to e^+e^-) = (6.77 \pm 0.32)$ keV [1],

$$\frac{g^2}{4\pi} = (2.02 \pm 0.10), \quad \text{or} \quad g = (5.04 \pm 0.12). \tag{2.41}$$

In the following, we always use this determination of g for numerical analysis.

C. Comparison with previous work

Before studying the full contents of our model, let us briefly consider the case $b = c = 0$, which is the same as the model described in Ref. [5]. For $c = 0$, we get the exact current-field identities and complete vector dominance from (2.14) and (2.15). Also, the symmetry relations (2.23)–(2.25) become

$$Z_\pi = \frac{m_\rho^2}{m_{a_1}^2}, \tag{2.42}$$

$$m_\rho^2 = \frac{g^2 f_\pi^2}{1 - Z_\pi}. \tag{2.43}$$

Therefore, in the case of $Z_\pi = 1/2$, we recover the usual KSFR relation (with $g = g_{\rho\pi\pi}$), and the results derived from Weinberg's sum rules in the single-pole approximations for $Z_\pi = 1/2$. However, one can easily convince oneself that the above equations overdetermine m_ρ, m_{a_1}, and g. For example, we consider three different cases which seem reasonable.

Case I. Assume that $g = g_{\rho\pi\pi} = 6.05$ determined from $\rho \to \pi\pi$. Then, $Z_\pi = 0.47$ and $m_{a_1} = 1.12$ GeV. (If we fix $g = g_{\rho\pi\pi} = 5.04$ from $\rho^0 \to e^+e^-$ instead, we would get $m_{a_1} = 0.970$ GeV, which is too small. So, we discard it.)

Case II. If we assume $Z_\pi = 1/2$, then $m_{a_1}^2 = 2m_\rho^2$ (Weinberg's sum rule) and $g = 5.85$.

Case III. If we use $m_{a_1} = 1.26$ GeV (PDG value) as an input, then $g = 6.54$.

For each case, one can choose κ_6 to get $g_{\rho\pi\pi} = 6.05$. The rates for processes involving the σ meson such as the widths for $\sigma \to \pi\pi$ and $a_1 \to \sigma\pi$ depend on the value b as well. In Table I, we show various physical quantities for each case with $b = c = 0$ (for which $m_\rho^2 = m_0^2$). The results do not compare with the data very well, especially for $a_1 \to \rho\pi$.

In previous work based on the nonlinear chiral Lagrangian with vector and axial vector mesons, this problem was avoided by including one more dimension-6 operator [11]:

TABLE I. Predictions with the κ_6 term and $b = c = 0$ for $m_\sigma = 1$ GeV (and 0.7 GeV in the parentheses). Three cases are explained in the text. Inputs are marked with a dagger for each case. The parameter κ_6 is adjusted to get the correct $g_{\rho\pi\pi}$ for each case.

	Case I	Case II	Case III	Data
g	$6.05^\dagger$	5.85	6.54	5.04
m_{a_1} (GeV)	1.12	$1.09^\dagger$	$1.26^\dagger$	1.26 ± 0.03
$\langle r^2 \rangle_\pi^{1/2}$	0.63 fm	0.64 fm	0.61 fm	(0.66 ± 0.01) fm
$\rho^0 \to e^+e^-$	4.70 keV	5.03 keV	4.02 keV	(6.77 ± 0.32) keV
$a_1 \to \rho\pi$	23 MeV	27 MeV	57 MeV	~ 400 MeV
f_D/f_S	-27%	-19%	-28%	$(-11.0 \pm 2.0)\%$
$a_1 \to \pi\gamma$	0.477 MeV	0.410 MeV	0.245 MeV	(0.640 ± 0.280) MeV
$\sigma \to \pi\pi$	310 MeV	424 MeV	168 MeV	(?)
	(102 MeV)	(139 MeV)	(57 MeV)	

$$\frac{\zeta_6}{2m_\rho^2}\ \mathrm{Tr}\ \left[l_{\mu\nu}\Sigma r^{\mu\nu}\Sigma^\dagger\right] \longrightarrow \frac{\zeta_6 f_0^2}{2m_\rho^2}\ \mathrm{Tr}\ \left[l_{\mu\nu}U r^{\mu\nu}U^\dagger\right]. \tag{2.44}$$

The analysis becomes more involved, since the ζ_6 term induces wave function renormalizations of $\boldsymbol{\rho}$ and $\mathbf{a}$ fields. The ζ_6 term does contribute to $a_1 \to \rho\pi$ and other processes. Adjustment of ζ_6 generally improves the results shown in Table I as discussed in [11]. Most of the numerical results presented in this paper in fact correspond to the $\zeta_6 = 0$ case, unless otherwise specified.

The importance of the κ_6 term can be seen from Table II, where various predictions with $\kappa_6 = 0$ are listed. The cases I, II are for $b = c = 0$, whereas the cases III and IV are for $b = 0$ and $c \neq 0$. Input assumptions are denoted by daggers, and symmetry relations, Eqs. (2.18)–(2.23), are used as before. Basically, we get too small $g_{\rho\pi\pi}$, or equivalently, too small a decay rate for $\rho \to \pi\pi$. Also, the decay rate for $a_1 \to \pi\gamma$ is always zero, since it is proportional to κ_6 as discussed in Sec. IV B [see Eq. (4.10)].

From Tables I and II we conclude that it is essential to keep both c and κ_6 terms to improve the phenomenology of π, ρ, a_1 system. Processes involving the σ meson constrain b, or equivalently, m_0^2, but give no hint as to the necessity of the c and κ_6 terms. The results for nonvanishing c, κ_6 are shown in Tables III–VI. We get better and simpler overall results. Relegating the details for each process to the following sections, we discuss the more general aspects of our model here.

First of all, the current-field identities are modified into

$$\mathbf{V}_\mu = \frac{m_\rho^2}{g}\,\boldsymbol{\rho}_\mu - 2cg\,\frac{f_\pi^2}{Z_\pi^2\, m_{a_1}^2}\,\boldsymbol{\pi}_r \times D_\mu \boldsymbol{\pi}_r - \frac{2cgf_\pi \boldsymbol{\pi}_r \times \mathbf{a}_\mu}{Z_\pi} + \cdots, \tag{2.45}$$

$$\mathbf{A}_\mu = \frac{m_{a_1}^2\, Z_\pi}{g}\,\mathbf{a}_\mu + f_\pi D_\mu \boldsymbol{\pi}_r + \cdots, \tag{2.46}$$

We note that $c = 0$ corresponds to the complete vector meson dominance in the $I = J = 1$ channel of the $\pi\pi$ system.

For $c \neq 0$, there are two solutions of c (or, equivalently, Z_π) as can be seen from Eqs. (2.20)–(2.23). For example, for $g = 5.04$ and $m_{a_1} = 1.26$ GeV, the two solutions are

$$(c, Z_\pi) = (-0.12, 0.17) \ \text{ or } \ (1.34, 0.83).$$

In Tables IV and V, we show predictions on the various processes for these two sets of solutions. The smaller solution for $|c|$ gives overall better phenomenology, which indicates that the vector dominance hypothesis is indeed a good approximation. So, we choose the smaller (c, Z_π) in the following sections.

One may worry that this c term would give a wrong value for the pion charge radius deduced from the vector form factor. We can easily verify that it is not the case. The matrix element of the vector current (2.45) between charged pions is given by

$$F_V(q^2) = \frac{m_\rho^2}{(m_\rho^2 - q^2)}\,\frac{1}{g}\,F_{\rho\pi\pi}(q^2) + \frac{2cg^2 f_0^2}{Z_\pi m_{a_1}^2}. \tag{2.47}$$

Thus, one gets

$$F_V(0) = \frac{1}{Z_\pi m_{a_1}^2}\,\left[m_\rho^2 + 2cg^2 f_0^2\right] = 1, \tag{2.48}$$

$$\langle r^2\rangle_\pi = \frac{6}{Z_\pi m_{a_1}^2}\left[1 - \frac{g^2 f_0^2}{2m_{a_1}^2} - \frac{\kappa_6 Z_\pi^2 m_{a_1}^2}{2m_\rho^2}\right] = \frac{6}{m_\rho^2}\,\frac{g_{\rho\pi\pi}}{g}. \tag{2.49}$$

In the above equations, we have used the symmetry relations, (2.20)–(2.24), and the definition of $g_{\rho\pi\pi}$, (2.30). Thus, we get

$$\langle r^2\rangle_\pi^{1/2} = \frac{\sqrt{6 \times 1.20}}{m_\rho} = 0.69 \ \text{ fm}, \tag{2.50}$$

which compares well with the experimental value (0.66 ± 0.01) fm. Note that the pure vector meson dominance (i.e., the $c = 0$ case and $g = g_{\rho\pi\pi}$) leads to $\langle r^2\rangle_\pi^{1/2} = \sqrt{6}/m_\rho = 0.63$ fm.

Also, we note that the κ_6 term has the same structure

TABLE II. Predictions without the κ_6 term ($\kappa_6 = 0$): the cases I, II are for $b = c = 0$, and the cases III and IV are for $b = 0, c \neq 0$, for $m_\sigma = 1$ GeV (and 0.7 GeV in the parentheses). Four cases are explained in the text. Inputs are marked with a dagger for each case. The relevant data can be found in the last column of Table I.

	Case I	Case II	Case III	Case IV
g	5.85	6.57	5.23	5.40
m_{a_1} (GeV)	$1.09^\dagger$	$1.26^\dagger$	$1.09^\dagger$	$1.26^\dagger$
$g_{\rho\pi\pi}$	4.39	4.50	$6.05^\dagger$	$6.05^\dagger$
$\rho \to \pi\pi$	80 MeV	84 MeV	152 MeV	152 MeV
$\langle r^2\rangle_\pi^{1/2}$	0.55 fm	0.52 fm	0.68 fm	0.67 fm
$\rho^0 \to e^+e^-$	5.03 keV	3.98 keV	6.29 keV	5.90 keV
$a_1 \to \rho\pi$	171 MeV	335 MeV	55 MeV	88 MeV
f_D/f_S	−2.3%	−5.2%	−2.3%	−5.2%
$a_1 \to \pi\gamma$	0.0 MeV	0.0 MeV	0.0 MeV	0.0 MeV
$\sigma \to \pi\pi$	424 MeV	149 MeV	2.8 MeV	4.5 MeV
	(139 MeV)	(50 MeV)	(1.7 MeV)	(0.7 MeV)

TABLE III. The $\pi\pi$ scattering lengths (a_l^I's) and the linear coefficients (b_l^I) in our model (with $m_0^2 = 0$), SU(2)×SU(2) chiral perturbation theory to $O(p^4)$ and the experimental data. Our predictions are essentially independent of m_0, m_{a_1}, and g, as long as the symmetry relations (2.18)–(2.23) hold.

	This work	SU(2) ChPT	Data
a_0^0	0.16	0.20	0.26 ± 0.05
b_0^0	0.20	0.24	0.25 ± 0.03
a_0^2	−0.045	−0.043	-0.028 ± 0.012
b_0^2	−0.092	−0.069	-0.082 ± 0.008
$2a_0^0 - 5a_0^2$	0.55	0.60	0.614 ± 0.028
a_1^1	0.034	0.038	0.038 ± 0.002

TABLE IV. Decay rates (in MeV) for a_1 and σ for $m_{a_1} = 1.26$ GeV, $(c, Z_\pi) = (-0.12, 0.17)$ and $m_\sigma = 1.0$ GeV, for four different values of m_0: $m_0^2/m_\rho^2 = 0.0, 0.2, 0.5, 1.0$, with $\zeta_6 = 0.0$. The values in parentheses are for $m_\sigma = 0.7$ GeV.

m_0^2/m_ρ^2	0.0	0.2	0.5	1.0	Data
$a_1 \to \rho\pi$	483	483	483	483	~ 400
f_D/f_S	7.8%	7.8%	7.8%	7.8%	−10.0%
$a_1 \to \pi\gamma$	0.670	0.670	0.670	0.670	(0.640 ± 0.280)
$\sigma \to \pi\pi$	528	211	3.4	373	(?)
	(166)	(68)	(1.8)	(106)	

TABLE V. Decay rates (in MeV) for a_1 and σ for $m_{a_1} = 1.26$ GeV, $(c, Z_\pi) = (1.34, 0.83)$ and $m_\sigma = 1.0$ GeV, for four different values of m_0: $m_0^2/m_\rho^2 = 0.0, 0.2, 0.5, 1.0$, with $\zeta_6 = 0.0$. The values in the parentheses are for $m_\sigma = 0.7$ GeV. [The larger c (or, Z_π) solution is chosen here.]

m_0^2/m_ρ^2	0.0	0.2	0.5	1.0	Data
$a_1 \to \rho\pi$	410	410	410	410	~ 400
f_D/f_S	−19%	−19%	−19%	−19%	−10.0%
$a_1 \to \pi\gamma$	1.31	1.31	1.31	1.31	(0.640 ± 0.280)
$\sigma \to \pi\pi$	2664	2586	2472	2287	(?)
	(837)	(813)	(778)	(721)	

TABLE VI. Predictions for $a_1 \to \pi\gamma$ of various approaches and the data.

Reference	$\Gamma(a_1 \to \pi\gamma)$	Assumptions
[18]	~ 2 MeV	CA, CVC, PCAC, VMD, Dispersion relation
[19]	1–1.4 MeV	Single quark transitions and VMD
[20]	1.4 MeV	Phenomenological approach and VMD
[21]	0.3 MeV	Hidden symmetry scheme
This work	0.670 MeV	Effective Lagrangian and VMD
[1,17]	0.640 ± 0.246 MeV	

TABLE VII. Dependences of $a_1 \to \rho\pi$ and $a_1 \to \pi\gamma$ on g. For each g, there are two values of ζ_6 which yield $\Gamma(a_1 \to \rho\pi)$ between 300 MeV and 500 MeV.

g	Z_ρ	$\Gamma(a_1 \to \rho\pi)$ (MeV)	$\Gamma(a_1 \to \pi\gamma)$ (MeV)
5.05	1.0	465	0.625
5.05	1.16	342	0.375
5.65	0.93	414	0.019
5.65	1.11	366	1.093
6.05	0.89	450	0.013
6.05	1.09	348	1.533

as the L_9 term in the $O(p^4)$ nonlinear chiral Lagrangian. In the chiral perturbation theory, the charge radius of a pion is given by

$$\langle r^2\rangle_\pi = \frac{12}{f_\pi^2} L_9 + (\text{chiral loops}), \tag{2.51}$$

so that our κ_6 corresponds to $L_9 = 7.3\times 10^{-3}$ neglecting loops. The parameter L_9 is determined essentially by the ratio $g_{\rho\pi\pi}/g$, or equivalently, $\rho\to\pi\pi$ and $\rho^0\to e^+e^-$.

Secondly, the symmetry relations for $c=0$, (2.42) and (2.43), are no longer true, and we have to go back to the original ones, (2.23)–(2.25). In view of (2.45) and (2.46), this would imply that saturation of Weinberg's sum rules with π,ρ, and a_1 is not good approximation, and that the contributions of $\pi\pi$ and $\pi\rho$ intermediate states to the spectral densities of vector and axial currents should be included. Thus, one can study deviations from simple assumptions such as complete vector dominance, saturation of Weinberg's sum rules using single pole approximations, and KSFR relation by allowing for nonzero c.

Furthermore, we have another free parameter b in (2.20) and (2.21). Therefore, we can even consider the case $m_0^2=0$, not considered in the earlier literature, in which the ρ meson acquires its mass entirely from the σ vacuum expectation value, i.e., through spontaneous chiral symmetry breaking. This case also gives vanishing amplitude for $a_1\to\sigma\pi$ for $\kappa_6=0$ independent of m_σ as discussed in Sec. IV C. We will occasionally examine the results of this interesting case below, although it turns out not to be favored phenomenologically, when all processes are considered.

For the purpose of numerical analysis, we use $g=5.04$ as determined from $\rho^0\to e^+e^-$. Then, we solve (2.23) for Z_π for given m_{a_1}, and then solve for c. We shall choose the value of Z_π which yields a c closer to 0, because the vector meson dominance hypothesis is a good first approximation. Then, we determine κ_6 to get the correct $g_{\rho\pi\pi}$. Finally, we can scan over m_0 from 0 to m_ρ^2 and determine b using (2.20). The relations between b and m_0^2 are shown in Fig. 1 for $m_{a_1}=1.26$ GeV and 1.09 GeV, respectively.

If one wants to use $g\simeq g_{\rho\pi\pi}$ and determine $g_{\rho\pi\pi}$ from KSFR relation or the ρ width, one necessarily has to include another dimension-6 operator, the ζ_6 term. We have scanned over ζ_6 to get a right order of magnitude for $a_1\to\rho\pi$, and calculated the corresponding decay width for $a_1\to\pi\gamma$. There are two solutions of ζ_6 (or equivalently, Z_ρ, defined in Appendix A) for each g. The results for three different values of g are shown in Table VII. It becomes difficult to correctly describe $a_1\to\pi\gamma$, as g gets larger. Therefore, it seems necessary to clearly distinguish g and $g_{\rho\pi\pi}$ when one considers the a_1 meson explicitly. This is a remnant of the modifications of interactions of pions with other particles and the KSFR relation as a result of the π-a_1 mixing and the finite mass effect of m_{a_1}.

In Sec. III A, we will find that the $\pi\pi$ scattering lengths are insensitive to m_0 as well as to the m_{a_1} and m_σ, as long as they satisfy the symmetry relations Eqs. (2.18)–(2.25).

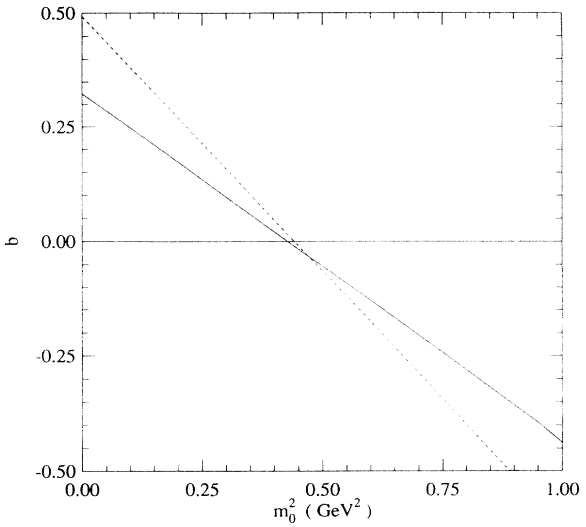

FIG. 1. The m_0^2 dependence of the parameter b for $m_{a_1}=1.26$ GeV (solid line) and $m_{a_1}=1.09$ GeV (dashed line).

This is due to the Nambu-Goldstone boson nature of pions, which basically determines the scattering lengths. However, some other quantities such as the width of σ and the decay rate for $a_1\to\sigma\pi$ are sensitive to the m_0, as discussed in the following sections.

III. $\pi\pi$ SCATTERING AND THE WIDTH OF σ

In this section, we consider in detail the effects of ρ and a_1 mesons on $\pi\pi$ scattering at low energy, and the important modification of the $\sigma\to\pi\pi$ width that can result.

A. The $\pi\pi$ scattering lengths

Let us first consider $\pi\pi$ scattering in our model:

$$\pi^a(p_a)+\pi^b(p_b)\to\pi^c(p_c)+\pi^d(p_d).$$

In general, the $\pi\pi$ scattering amplitude can be written as

$$\begin{aligned}\mathcal{M}_{ab;cd} = {}& A(s,t,u)\ \delta_{ab}\delta_{cd} + A(t,s,u)\ \delta_{ac}\delta_{bd}\\ & + A(u,t,s)\ \delta_{ad}\delta_{bc},\end{aligned} \tag{3.1}$$

and it suffices to give the expression for $A(s,t,u)$. It can be further decomposed into amplitudes (T^I) with definite total isospin $I=0,1,2$ of the two incoming pions:

$$\begin{aligned}T^0(s,t,u) &= 3A(s,t,u)+A(t,s,u)+A(u,t,s),\\ T^1(s,t,u) &= A(t,s,u)-A(u,t,s),\\ T^2(s,t,u) &= A(t,s,u)+A(u,t,s).\end{aligned} \tag{3.2}$$

Each T^I can be expanded in terms of partial waves as

$$T^I(s,t,u) = 32\pi \sum_{l=0}^{\infty}(2l+1)\, t_l^I(s)\, P_l(\cos\theta), \qquad (3.3)$$

where l is the relative orbital angular momentum of the pions and θ is the scattering angle in the center of momentum frame.

For each l and I, the phase shift is defined as

$$t_l^I = \frac{1}{2q}\,\frac{1}{2i}\left[e^{2i\delta_l^I(s)} - 1\right], \qquad (3.4)$$

where

$$q = \sqrt{\frac{s}{4m_\pi^2} - 1} \qquad (3.5)$$

is the magnitude of the three-velocity of a pion in the center of momentum frame. In the limit of $q \to 0$, the real part of t_l^I becomes

$$\mathrm{Re}\; t_l^I(s) \approx q^{2l}\left[\, a_l^I + b_l^I q^2 + O(q^4)\,\right], \qquad (3.6)$$

which defines the $\pi\pi$ scattering length a_l^I and the linear coefficient b_l^I. Both a_l^I and b_l^I are dimensionless in our definitions.

The original linear σ model gives the well known result for the $\pi\pi$ scattering amplitude:

$$A(s,t,u) = -2\lambda\left[1 - \frac{2\lambda f_0^2}{m_\sigma^2 - s}\right]. \qquad (3.7)$$

This by itself satisfies the Adler consistency condition, $A(m_\pi^2, m_\pi^2, m_\pi^2) = 0$ with $Z_\pi = 1$, by virtue of Eq. (2.19).

In our model, $\pi\pi$ scattering occurs through the Feynman diagrams shown in Fig. 2. Here, we have the ρ meson exchanges, the π-a_1 mixing and the wave function renormalization of the pion field in addition to the above amplitude, Eq. (3.7). Evaluating the Feynman diagrams in Figs. 2(a) and 2(b) using (A12)–(A14), we get

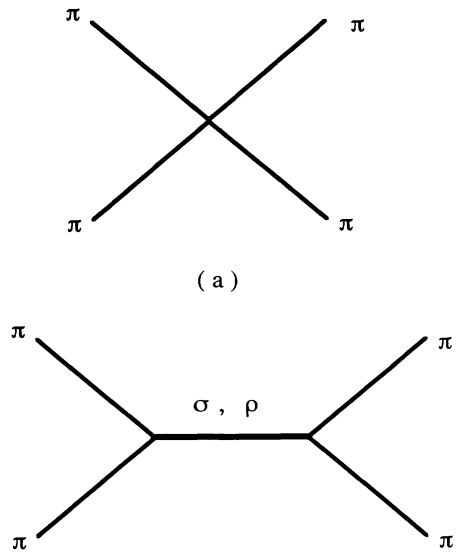

FIG. 2. Feynman diagrams contributing to the $\pi\pi$ scattering: (a) π^4 interaction and (b) σ and ρ exchanges. Here, the $\rho\pi\pi$ and $\sigma\pi\pi$ vertices contain all the contributions from the π-a_1 mixing and/or the κ_6 term.

$$A(s,t,u) = A_{\pi^4}(s,t,u) + A_\sigma(s,t,u) + A_\rho(s,t,u), \qquad (3.8)$$

where

$$A_{\pi^4}(s,t,u) = \frac{1}{Z_\pi^2}\left[-2\lambda + \frac{g^4 f_0^2}{Z_a^2 m_{a_1}^4}\left\{(1+2c)\, s - 2(b-c)\,(s - 2m_\pi^2)\right\}\right], \qquad (3.9)$$

$$A_\sigma(s,t,u) = \frac{1}{Z_\pi^2}\left(\frac{f_0^2}{m_\sigma^2 - s}\right)\left[2\lambda - \frac{g^2}{Z_a m_{a_1}^2}\left\{\left(1 + \frac{m_0^2}{Z_a m_{a_1}^2}\right)s - \frac{2m_\pi^2 m_0^2}{Z_a m_{a_1}^2}\right\}\right]^2, \qquad (3.10)$$

$$A_\rho(s,t,u) = \left(\frac{s-u}{m_\rho^2 - t}\right)\left[F_{\rho\pi\pi}(t)\right]^2 + (t \leftrightarrow u). \qquad (3.11)$$

To obtain the scattering length and the linear coefficient, we make the following substitutions in Eq. (3.2), get $t_l^I(s)$ using Eq. (3.3), and then expand t_l^I around $q = 0$:

$$s = 4m_\pi^2\,(q^2+1),$$
$$t = -2m_\pi^2\, q^2\,(1 - \cos\theta),$$
$$u = -2m_\pi^2\, q^2\,(1 + \cos\theta).$$

In Table III, we list the $\pi\pi$ scattering lengths a_l^I's and the linear coefficients b_l^I's in our model along with the exeprimental data. The results from the SU(2) chiral perturbation theory [13] are also shown for comparison. Our results depend on m_0, m_σ, m_{a_1}, and g in general, but not very much. The numbers shown in Table III are for $m_0 = 0, m_\sigma = m_\rho$ and $g = 5.04$. Therefore, $m_0^2 = 0$ is as good as $m_0^2 = m_\rho^2$ from the $\pi\pi$ scattering data. This is not altogether unexpected: the low-energy theorems for $\pi\pi$ scattering follow from current algebra and PCAC only, which are not sensitive to the relative contributions of m_0^2, b, and c terms to the vector and axial vector meson masses, or the particular choice of m_{a_1}, as long as all contributions to the amplitude are included and the full set of symmetry relations (2.18)–(2.25) consistently taken into account.

B. The width of the σ

Another important consequence of our model is that it can lead to a sizable reduction of the $\sigma \to \pi\pi$ decay width, as compared to original expectations. It is well known that the original linear σ model predicts

$$\Gamma(\sigma \to \pi\pi) = \frac{3}{8\pi}\,(2\lambda f_\pi)^2\,\frac{|\mathbf{p}_\pi|}{2m_\sigma^2}, \tag{3.12}$$

with $m_\sigma^2 = 2\lambda f_\pi^2$. Thus, we would have $\Gamma(\sigma \to \pi\pi) \approx$ 1650 MeV and 760 MeV for $m_\sigma = 1$ GeV and $m_\sigma = m_\rho$, respectively. This width is, therefore, typically larger than the mass, which makes it difficult to identify the σ meson with any known state.

In our model, the width of σ is altered by the $\pi - a_1$ mixing, and can be significantly smaller compared to the original linear σ model. Specifically, the amplitude for $\sigma \to \pi\pi$ in our model is obtained from (A14):

$$\begin{aligned}\mathcal{M}(\sigma \to \pi^a\pi^b) &= \delta_{ab}\,\frac{f_0}{Z_\pi}\left\{-2\lambda + \frac{g^2}{Z_a m_{a_1}^2}\left[\left(1 + \frac{m_0^2}{Z_a m_{a_1}^2}\right) m_\sigma^2 - \frac{2m_\pi^2 m_0^2}{Z_a m_{a_1}^2}\right]\right\} \\ &\equiv \delta_{ab}\, G_{\sigma\pi\pi}(m_\sigma^2).\end{aligned} \tag{3.13}$$

The relevant Feynman diagrams are shown in Fig. 3. This is rather sensitive to g and m_0, as well as m_σ. The first term in the above amplitude is the usual $\sigma\pi^2$ interaction given by the potential in the linear σ model, whereas the second term is induced by the π-a_1 mixings in the kinetic term for the π fields and in the b, c terms. These two interfere destructively as indicated by the opposite signs in (3.13), and the σ width can be considerably smaller than the one predicted by the original σ model.

In Figs. 4(a) and 4(b) we show the m_0 dependence of the σ width for $m_\sigma = 1.0$ GeV and $m_\sigma = 0.7$ GeV, respectively. We note that for $g = 5.04$, a width of 500 MeV or so, with $m_\sigma 1$ GeV (as suggested in Ref. [2]) can cor-

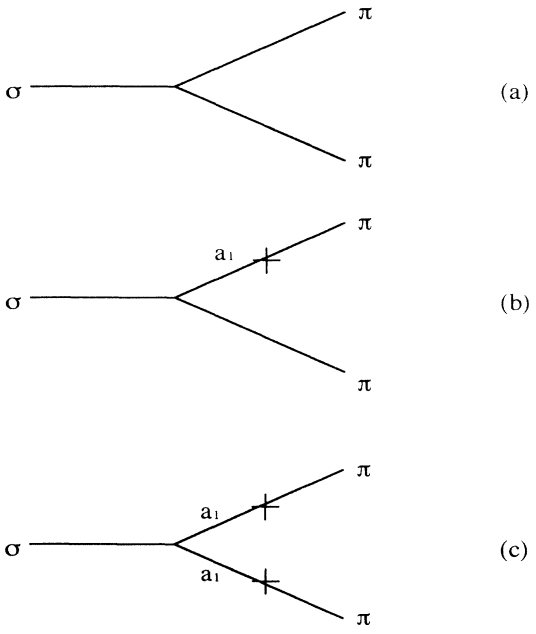

FIG. 3. Feynman diagrams contributing to $\sigma \to \pi\pi$ including the π-a_1 mixing: (a) from the potential $\propto \lambda$, (b) from the $\mathcal{L}_{\rm kin}(\sigma)$, and (c) from the $\mathcal{L}_{\rm kin}(\pi)$ and the b, c terms.

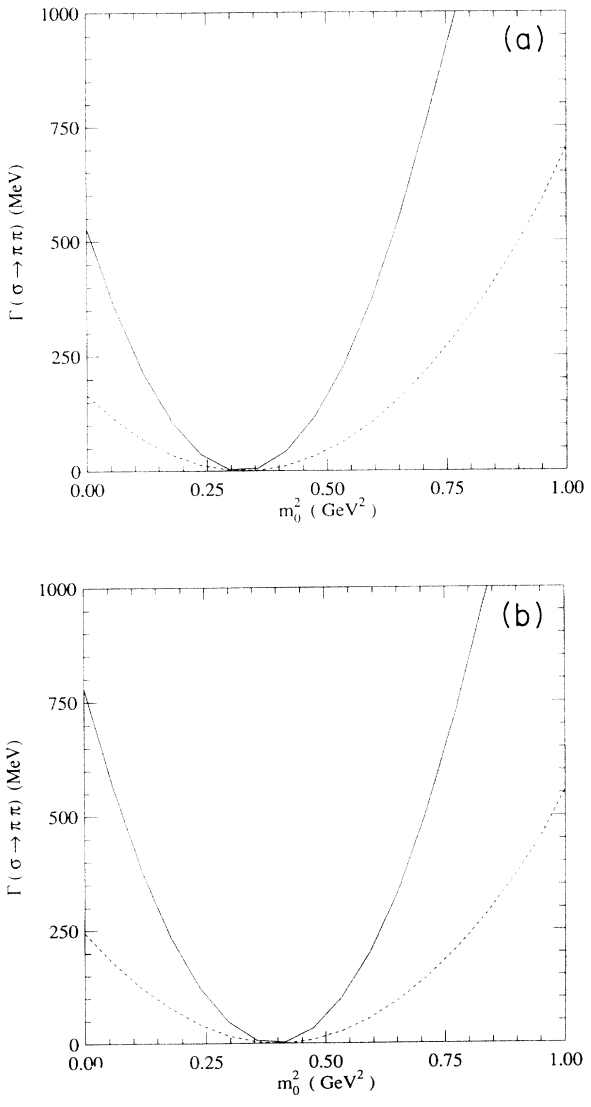

FIG. 4. The m_0 dependence of $\Gamma(\sigma \to \pi\pi)$ for $m_\sigma = 1$ GeV (solid curve) and $m_\sigma = 0.7$ GeV (dashed curve): (a) $m_{a_1} = 1.26$ GeV, and (b) $m_{a_1} = 1.09$ GeV.

respond to values for m_0^2 around $m_0^2 \simeq 0$ and $m_0^2 \simeq m_\rho^2$. We emphasize that the latter possiblility differs here from previous treatments in the literature in that we have then $b \simeq c \neq 0$. We see that $\pi - a_1$ mixing effects lead in this case to a reduction in the $\sigma \to \pi\pi$ width by a factor of 3, as compared to the value that would be inferred from the usual formula (3.12). Even more drastic reductions are possible, as seen in the figures. To determine which values of m_0^2 are to be favored, we will examine in Sec. IV C the magnitude of the non-$\rho\pi$ decay width of the a_1, known from experiment to be rather small when compared to the dominant $a_1 \to \rho\pi$ process.

Finally, we comment on the previously considered case $m_0 = m_\rho$, with $b = c = 0$ as an additional constraint: we emphasize once again that this does not lead to a good overall phenomenology. Still, we see from Table I that $\pi - a_1$ mixing effects on the σ width can be sizable: we can also use $g = 5.04$ to fit $\rho^0 \to e^+e^-$ and then the $\sigma \to \pi\pi$ is reduced to $\simeq 812$ MeV for $m_\sigma = 1$ GeV.

IV. PHENOMENOLOGY OF A_1 MESON

A. $a_1 \to \rho\pi$

The effective Lagrangian constructed in the previous sections can be shown to reproduce the current algebra and PCAC result on $a_1\rho\pi$ coupling. Let us parametrize the amplitude for $a_1(k,\epsilon) \to \rho(k',\epsilon') + \pi(p)$ as

$$\mathcal{M}(a_1 \to \rho\pi) = f_{a_1\rho\pi}\, \epsilon\cdot\epsilon' + g_{a_1\rho\pi}\, k'\cdot\epsilon\, k\cdot\epsilon'. \quad (4.1)$$

The interaction Lagrangian (A15) yields the form factors for $a_1 \to \rho\pi$ (with $\zeta_6 = 0$):

$$f_{a_1\rho\pi}(k^2,k'^2) = \frac{g^2 f_\pi}{Z_\pi}\left[2c + \frac{k'^2}{m_{a_1}^2}\right] + \frac{\kappa_6 g^2 f_\pi}{m_\rho^2}\, p\cdot k', \quad (4.2)$$

$$g_{a_1\rho\pi}(k^2,k'^2) = -\frac{\kappa_6 g^2 f_\pi}{m_\rho^2}, \quad (4.3)$$

which agree with an expression given in Ref. [5] if we set $c = 0$. For $\kappa_6 = 0$ and any c, the form factor $f_{a_1\rho\pi}$ can be written as

$$f_{a_1\rho\pi}(m_{a_1}^2, m_\rho^2) = \frac{Z_\pi}{f_\pi}\,(m_{a_1}^2 - m_\rho^2), \quad (4.4)$$

using Eqs. (2.23) and (2.24). This is nothing but the result derived by Geffen, and Brown and West using the current algebra and PCAC technique [14]. We note that Eq. (4.4) holds even for nonvanishing c in our model, while the original derivations by Geffen, and Brown and West were done with $c = 0$ (complete vector meson dominance). The overall factor Z_π was obtained in Ref. [14] by including $\rho\pi$ contributions. In our approach with the effective Lagrangian based on the massive Yang-Mills gauge theory, the Z_π factor results from the non-Abelian nature of the ρ, a_1 interactions. More specifically, the Z_π factor is derived by the triple gauge boson (ρ-a_1 - a_1) interaction in the kinetic energy term in the non-Abelian gauge theory and the π-a_1 mixing. We note, however, that the κ_6 term, missing from (4.4), is of crucial importance in reproducing the correct $\rho \to \pi\pi$ width and $a_1 \to \pi\gamma$, as shown in Table II.

For $g = 5.04$ and $m_{a_1} = 1.26$ GeV, the width becomes

$$\Gamma(a_1 \to \rho\pi) \approx 483 \ \text{MeV}. \quad (4.5)$$

Hence, the width for $a_1 \to \rho\pi$ for $m_{a_1} = 1.26$ GeV comes out right in our model. $\Gamma(a_1 \to \rho\pi)$ is rather sensitive to m_{a_1} and the $\rho^0 - \gamma$ coupling g, as shown in Fig. 5. The solid, the dashed and the dotted curves are for $g = 5.04$ and 5.04 ± 0.12, respectively. The main uncertainty in our prediction comes from the value of g as well as from the value of m_{a_1}. For example, we get $\Gamma(a_1 \to \rho\pi) = 97$ MeV for $m_{a_1} = \sqrt{2}\, m_\rho = 1090$ MeV.

One can also write the above amplitude (4.1) in terms of the S- and D- wave amplitudes for the final $\rho\pi$ system [15]

$$f^S_{a_1\rho\pi} = \frac{\sqrt{4\pi}}{3m_\rho}\left[(E_\rho + 2m_\rho)\, f_{a_1\rho\pi} + \mathbf{k}'^2 m_{a_1} g_{a_1\rho\pi}\right], \quad (4.6)$$

$$f^D_{a_1\rho\pi} = -\frac{\sqrt{8\pi}}{3m_\rho}\left[(E_\rho - m_\rho)\, f_{a_1\rho\pi} + \mathbf{k}'^2 m_{a_1} g_{a_1\rho\pi}\right]. \quad (4.7)$$

In our case, the (D/S) ratio is about $+7\%$ compared to $(-11.0 \pm 2.0)\%$ [16]. The experimental value was extracted from $\tau \to 3\pi$ decay assuming Isgur's flux tube model, which is quite different from ours. Therefore, this disagreement may not be a serious one.

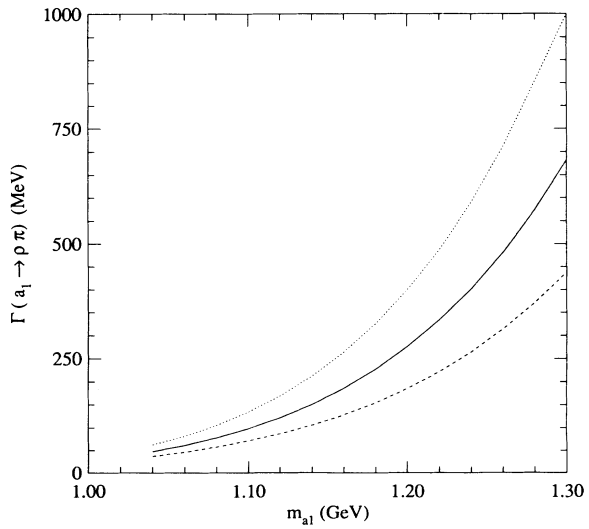

FIG. 5. The m_{a_1} dependences of $\Gamma(a_1 \to \rho\pi)$ for $g = 5.04 \pm 0.12$. The solid, the dashed, and the dotted curves are for $g = 5.04, 5.16, 4.92$, respectively.

B. $a_1^{\pm} \to \pi^{\pm}\gamma$

One can also study the radiative decay process $a_1^{\pm} \to \pi^{\pm}\gamma$ using the above form factors Eqs. (4.2) and (4.3) for $k'^2 = 0$ in conjunction with the idea of vector meson dominance of hadronic electromagnetic current, Eq. (2.38). This decay receives from both $\rho^0 - \gamma$ mixing and the direct coupling to the photon [from the first and the last terms in Eq. (2.45), respectively]. After adding these two contributions, one finds that only the κ_6, ζ_6 terms in $f_{a_1\rho\pi}$ form factor contribute to $a_1^{\pm} \to \pi^{\pm}\gamma$:

$$\mathcal{M}(a_1^+(k,\epsilon) \to \pi^+(p)\gamma(k',\epsilon')) = \frac{e\sqrt{Z_\rho}}{g}\,\epsilon\cdot\epsilon'\left[f_{a_1\rho\pi}(k'^2=0) - \frac{2cg^2 f_0}{\sqrt{Z_a Z_\rho Z_\pi}}\right]. \tag{4.8}$$

For $\zeta_6 = 0$, the result is

$$\mathcal{M}(a_1^+(k,\epsilon) \to \pi^+(p)\gamma(k',\epsilon')) = \epsilon\cdot\epsilon'\,\frac{\kappa_6 e g f_\pi}{m_\rho^2}\,p\cdot k', \tag{4.9}$$

so that the amplitude is proportional to κ_6. For $m_{a_1} = 1.26$ GeV, we then obtain

$$\Gamma(a_1^{\pm} \to \pi^{\pm}\gamma) = 670 \text{ keV}, \tag{4.10}$$

which is consistent with the PDG value (640 ± 246) keV [1,17]. This serves to highlight the importance of the κ_6 term, as it allows for the observed decay $a_1 \to \pi\gamma$, as well as increasing the $\rho\pi$ decay width of the a_1, and accounting for the difference between $g_{\rho\pi\pi}$ and g. This decay is also very sensitive to m_{a_1} and g as shown in Fig. 6. The m_{a_1} dependence is mainly due to kinematical reason, whereas the sensitivity on g comes from implicit dependence of κ_6 on m_{a_1} through (2.29). Had we used $m_{a_1} = 1.20$ GeV, the rate would be 367 keV with $\Gamma(a_1 \to \rho\pi) = 276$ MeV.

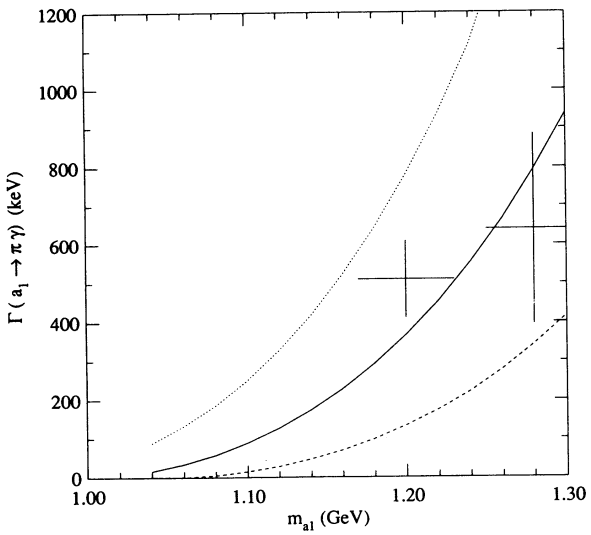

FIG. 6. The m_{a_1} dependences of $\Gamma(a_1 \to \pi\gamma)$ for $g = 5.04 \pm 0.12$. The solid, the dashed, and the dotted curves are for $g = 5.04, 5.16, 4.92$, respectively.

For comparison, we quote previous predictions on the decay rate for $a_1 \to \pi\gamma$. Calculations based on current algebra, CVC, and unsubtracted dispersion relation [18] predict it to be about 2 MeV which may be too large. A model [19] based on the single quark transition along with the vector dominance hypothesis in $a_1 \to \pi\gamma$ predict $\Gamma(a_1 \to \pi\gamma) = 1 - 1.6$ MeV, for $m_{a_1} = 1.2$ GeV and $\Gamma(a_1 \to \rho\pi) \sim 300$ MeV. Another group uses the phenomenological Lagrangian for $a_1 - \rho$-π vertex and the idea of vector meson dominance [20] to predict $\Gamma(a_1 \to \pi\gamma) = 1.42$ MeV for $m_{a_1} = 1.26$ GeV and $\Gamma(a_1 \to \rho\pi) = 400$ MeV. If a_1 meson is regarded as a gauge boson in the extended hidden symmetry [21], one finds that $\Gamma(a_1 \to \rho\pi) = 360$ MeV and $\Gamma(a_1 \to \pi\gamma) = 0.3$ MeV for $m_{a_1} = \sqrt{2}m_\rho = 1.09$ GeV. Thus, our result is at the lower range of magnitude compared to other predictions, and in better agreement with the data. This is one of the firm predictions of our model as constructed in Sec. II. Especially, our result manifestly respects all the important properties such as spontaneously broken chiral symmetry, chirally symmetric interactions among particles under consideration, the idea of (nearly) complete vector meson dominance. Also, it remains intact in the limit of the nonlinear σ model (i.e., in the limit of $m_\sigma \to \infty$).

Although the above amplitude (4.8) does not look gauge invariant, one can explicitly check that it actually is. The most direct way to verify this is to go back to the original Lagrangian, and replace ρ_μ^0 by eB_μ/g [$\rho-\gamma$ mixing given by (2.38)]. Then, the masslike b, c terms drop out as before, and (A15) contains only $B_{\mu\nu}$. Thus, the resulting ampitude is gauge invariant. More specifically, we can derive the following for the on-shell photon (a_1 can be either real or virtual),

$$\mathcal{L}(a_1\pi\gamma) = \frac{\kappa_6 e g f_\pi}{m_\rho^2}\,B_{\mu\nu}\,(\mathbf{a}^{\mu\nu}\times\boldsymbol{\pi})_3, \tag{4.11}$$

by doing partial integration on (A15) with $\zeta_6 = 0$. This is manifestly gauge invariant, and proportional to κ_6.

C. $a_1 \to \sigma\pi \to (\pi\pi)_s\pi$

Another interesting consequence of our effective Lagrangian is that one can accommodate a rather small partial width for the process $a_1 \to (\pi\pi)_s\pi$, including a contribution due to the process $a_1 \to \sigma\pi$. In our model, the amplitude for this process is given by Eq. (A16):

$$\mathcal{M}(a_1(k,\epsilon) \to \sigma(p_\sigma)\pi(p_\pi)) = -\frac{ig}{\sqrt{Z_{a_1}Z_\pi}}\left[\frac{2m_0^2}{Z_a m_{a_1}^2} - \kappa_6 Z_\pi\,\frac{m_{a_1}^2}{m_\rho^2}\right]\epsilon\cdot p_\pi, \equiv G_{a_1\sigma\pi}\,\epsilon\cdot p_\pi. \tag{4.12}$$

It is interesting to note that the amplitude for $a_1 \to \sigma\pi$ vanishes identically in the special case $m_0^2 = \kappa_6 = 0$ (i.e., keeping only operators of dimension four or less), and this, for any value of m_{a_1} and m_σ. We have argued, however, that it is necessary to take $\kappa_6 \neq 0$.

With the κ_6 term and for arbitrary m_0^2, one can get the decay rate for $a_1 \to \sigma\pi$. The result is sensitive to m_σ as well as m_0^2, simply for kinematical reasons. For $m_{a_1} = 1.26$ GeV and $m_\sigma = 1$ GeV, we get, for example,

$$\Gamma(a_1 \to \sigma\pi) = 0.2 \ \ (3.5) \ \ \text{MeV}, \tag{4.13}$$

for $m_0 = m_\rho$ (0 GeV), respectively: $m_0 = m_\rho$ corresponds to $b = c \neq 0$.

However, a discussion of the non$-\rho\pi$ decays of a_1 must also include the direct decay $a_1 \to 3\pi$. In our model, the final 3π state is reached by three independent intermediate states as shown in Figs. 7(a) and 7(b). If we use narrow width approximation for ρ, the total width for $a_1 \to 3\pi$ can be approximated as [22]

$$\Gamma(a_1 \to 3\pi) \approx \Gamma(a_1 \to \rho\pi) + \Gamma(a_1 \to 3\pi)_{\text{non-}\rho\pi}, \tag{4.14}$$

where the second part is due to the $\sigma\pi$ intermediate state and the direct $a_1 \to 3\pi$ transition given by (A17).

The amplitude for $a_1^+ \to (\pi\pi\pi)^+_{\text{non}-\rho\pi}$ can be parametrized as

$$\mathcal{M}(a_1^+(k,\epsilon) \to \pi^+(p_1)\pi^+(p_2)\pi^-(p_3))_{\text{non-}\rho\pi} \equiv \epsilon(k)\cdot p_3 \; G_1^{\text{tot}} + \epsilon(k)\cdot p_1 \; G_2^{\text{tot}}, \tag{4.15}$$

where p_3 is the four-momentum of the odd pion. We relegate explicit expressions for two-form factors $G_{1,2}^{\text{tot}}$'s to Appendix B, except a remark that they depend on m_0^2. Thus, the non-$\rho\pi$ decay width for $a_1 \to 3\pi$ is a sensitive function of m_0^2, whereas $a_1 \to \rho\pi$ is not at all.

Now, it is straightforward to get the non$-\rho\pi$ decay rate of $a_1 \to 3\pi$ from the above amplitude. Combining with the width for $a_1 \to \rho\pi$ obtained in Sec. IV A, one can calculate the branching ratio for $a_1 \to \rho\pi$. The result is a sensitive function of m_0, as shown in Fig. 8 for $m_{a_1} = 1.26$ GeV. The solid and the dashed curves correspond to two values of m_σ: $m_\sigma = 1$ GeV (the solid curve) and 0.7 GeV (the dashed curve), respectively. Recent data from ARGUS Collaboration suggest that the non$-\rho\pi$ contribution to the 3π final state is less than 6% at the 95% CL.

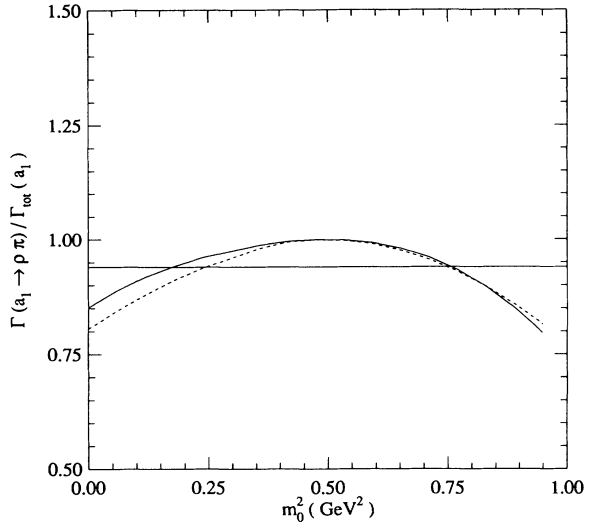

FIG. 8. The m_0^2 dependence of the branching ratio of $a_1 \to \rho\pi$ for $m_{a_1} = 1.26$ GeV. The solid and the dashed curves are for $m_\sigma = 1.0$ GeV and 0.7 GeV, respectively.

Taking this observational constraint into account further limits the possible values of m_0^2. From Fig. 8, we get, for $m_{a_1} = 1.26$ GeV and $m_\sigma = 1$ GeV,

$$0.17 \ \text{GeV}^2 \leq m_0^2 \leq 0.77 \ \text{GeV}^2. \tag{4.16}$$

Next, another look at Fig. 4(a) indicates that the low values of m_0^2 are probably excluded: we should bear in mind, however, that the results in Fig. 8 are based on the rather crude approximation (4.14) which should certainly be improved. We note finally that for $m_{a_1} = 1.09$ GeV, the non-$\rho\pi$ contribution to the a_1 width as calculated here always exceeds 10% for all values of m_0^2, which is inconsistent with data.

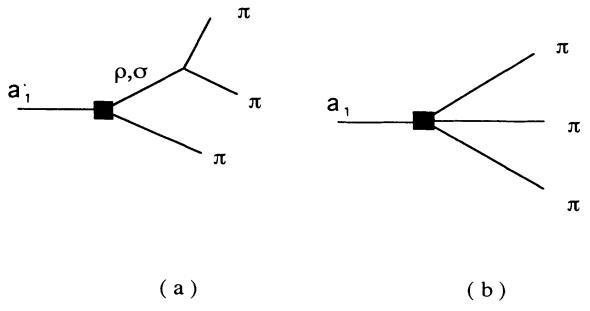

FIG. 7. Feynman diagrams contributing to $a_1 \to (\pi\pi)_s\pi$: (a) ρ, σ contribution and (b) direct transition. All the vertices include the contributions from the $\pi - a_1$ mixing and/or the κ_6 term.

V. THE WESS-ZUMINO ANOMALY IN THE LINEAR σ MODEL

So far, we have considered only processes with normality[4] conservation. To describe anomalous processes such as $\pi^0 \to \gamma\gamma$ or $\omega \to \pi^0\rho^0 \to \pi^0\gamma$, we need terms with the Levi-Civita tensor, a generalization of the Wess-Zumino anomaly, with correct transformation

[4]Normality for a meson with J^{PC} is defined to be $P(-1)^J$. Therefore, the photon, ρ, ω, and σ have even normality, while π, K, and a_1 are odd.

properties under local chiral transformations. Since the SU(2) group is anomaly-free, one has to extend the chiral group to $SU(3)_L \times SU(3)_R$, and the ω is included by redefining l_μ, r_μ as

$$l_\mu \to l_\mu + \frac{1}{2}\,\omega_\mu,$$
$$r_\mu \to r_\mu + \frac{1}{2}\,\omega_\mu.$$

The $\omega - \gamma$ mixing is obtained by replacing

$$\omega_\mu \to \omega_\mu - \frac{e}{3g} B_\mu$$

in the masslike terms, as in Sec. II B.

The anomaly is a manifestation of the fact that chiral symmetry cannot be retained in the quantized theory of fermions coupled to gauge fields. Under local $SU(3)_L \times SU(3)_R$ chiral transformations, the effective action transforms as

$$\delta\Gamma_{LR}[\Sigma, l, r] = -\frac{N_c}{24\pi^2}\int_{M^4} d^4x \times \left\{\epsilon_L\left[(dl)^2 - \frac{i}{2}dl^3\right] - (L \leftrightarrow R)\right\}, \tag{5.1}$$

where N_c is the number of colors and the right-hand side of this equation is obtained at the quark level. The explicit form of Γ_{LR} can be conveniently written in terms of differential forms:

$$\Gamma_{LR}[\Sigma, l, r] = C\int_{M^5} d^5x\ \mathrm{Tr}[\overline{\alpha}^5] + (\text{covariantization}) \tag{5.2}$$

where we have defined

$$C = -\frac{iN_c}{240\pi^2} \tag{5.3}$$

and

$$\overline{\alpha} \equiv d\Sigma\Sigma^{-1}, \tag{5.4}$$

which transforms as $\overline{\alpha} \to L\overline{\alpha}L^\dagger$ under *global* chiral transformations. The functional Γ_{LR} can be constructed along the same lines as followed in Refs. [23]. In fact, one can make the following substitutions in the results of Refs. [23]:

$$U \to \frac{1}{f_0 + s}\,\Sigma, \tag{5.5}$$

$$\alpha \equiv dUU^{-1} \to \overline{\alpha} \equiv \alpha + \frac{ds}{f_0 + s}, \tag{5.6}$$

$$\beta \equiv U^{-1}dU \to \overline{\beta} \equiv \Sigma^{-1}d\Sigma = \beta + \frac{ds}{f_0 + s}. \tag{5.7}$$

These follow from the fact that the left- and right-hand sides have the same transformation properties under *local* as well as *global* chiral transformations.

To maintain the conservation of the vector current, at the expense of that of the axial vector current, we consider Bardeen's form of the anomaly. Then, the corresponding functional is obtained by

$$\Gamma_{WZ} = \Gamma_{LR}[\Sigma, l, r] - \Gamma[\Sigma = (f_0 + s), l, r]. \tag{5.8}$$

We note that one can easily recover the results of Ref. [23] (the gauged Wess-Zumino anomaly) by taking $s = 0$.

Thus, one can have the $\omega\rho\pi$ coupling in the *linear* σ model, which would describe $\omega \to \pi^0\gamma$ and $\pi^0 \to \gamma\gamma$ upon introducing a photon field through ρ-γ and ω-γ mixings as usual. Proceeding as in previous work [23], we only write down the $\omega\rho\pi$ coupling

$$\mathcal{L}(\omega\rho\pi) = -\frac{3g^2}{8\pi^2 f_\pi}\,\epsilon_{\mu\nu\alpha\beta}\,\partial^\mu\omega^\nu\,\partial^\alpha\boldsymbol{\rho}^\beta \cdot \boldsymbol{\pi}_r, \tag{5.9}$$

which can be used in the old Gell-Mann–Sharp–Wagner model [24] for meson decays. For example, we can describe the decay $\omega \to \pi^0\gamma$ through ρ-γ mixing:

$$\Gamma(\omega \to \pi^0\gamma) = \frac{3\alpha g^2}{64\pi^4 f_\pi^2}\,|\mathbf{p}_\pi|^3 \approx \left(\frac{g}{6}\right)^2 802\ \text{keV}. \tag{5.10}$$

Thus, we get $\Gamma(\omega \to \pi^0\gamma) = (566 \pm 27)$ keV using[5] $g = (5.04 \pm 0.12)$, whereas the experimental data are (717±43) keV.

VI. CONCLUSIONS

In this paper, we have studied the properties of π, ρ, a_1, and σ mesons in an extended linear σ model. The vector and axial vector mesons were included, as usual, as phenomenological gauge fields associated with the *local* chiral symmetry, a technical device that leads to field-current identities once this local chiral symmetry is explicitly broken down to the global symmetry by adding nongauge invariant (but globally invariant) terms quadratic in the vector fields to the Lagrangian. A novel feature of our work is the inclusion of the b and c terms, in addition to the usual bare mass term (m_0^2) for the vector and axial-vector mesons.

Our results are presented in Tables III, IV, and VI for the particular choice of $m_{a_1} = 1.26$ GeV, and they are in good agreement with the available data except for the D/S ratio f_D/f_S in $a_1 \to \rho\pi$ decay: we note, however, that the extraction of this parameter appears to be unusually model dependent. In particular, we obtain correct $\pi\pi$ low-energy scattering lengths, as a result of the consistent inclusion of all ρ and a_1 effects, in a manner respecting the global chiral symmetry. Our prediction for the $a_1 \to \rho\pi$ width is close to the experimental result,

[5]Note that we distinguish g from $g_{\rho\pi\pi}$. If we used $g \simeq g_{\rho\pi\pi} = 6.05$ as usually done, we would get $\Gamma(\omega \to \pi^0\gamma) = 815$ keV. This amounts to neglecting effects induced by the a_1 meson.

even considering the various uncertainties involved in the extraction of a_1 resonance parameters for $\tau \to 3\pi\nu_\tau$ decay. The decay $a_1^\pm \to \pi^\pm\gamma$ is successfully described in our model, which is contrasted with other approaches in Table VI. The fact that non$-\rho\pi$ contributions to $a_1 \to 3\pi$ decay appear greatly suppressed can be accommodated as a constraint on the acceptable range for the parameter m_0^2 in our model. Most remarkably, the $\sigma \to \pi\pi$ width can be considerably smaller than that predicted in the original σ model without vector mesons as a result of the effect of $\pi-a_1$ mixing, and given the range of possible values for m_0^2. This result is important in that it addresses the single most quoted objection to considering the linear σ model as a serious starting point for phenomenology, namely, the difficulty of identifying the σ meson with the scalar isoscalar state around 1 GeV that appears in the Particle Data Group [1] tables. It is clear, however, that for the purposes of more detailed phenomenology, an extension of the present model to $SU(3)_L \times SU(3)_R$ and to include a scalar glueball (in a manner consistent with the QCD trace anomaly) will be required.

ACKNOWLEDGMENTS

We are grateful to S. Gasiorowicz, J.L. Rosner, and M. Voloshin for discussions on the subject. P.K. thanks the Aspen Center for Physics for support and hospitality, where a part of this work was done. This work was supported in part by DOE Grant No. DE-AC02-83ER-40105.

APPENDIX A: INTERACTION LAGRANGIANS

In this appendix, we give the full expressions for our model Lagrangian constructed in Sec. II, and collect various interaction Lagrangians relevant to processes we discuss in the text. They are obtained from Eqs. (2.13), (2.28), and (2.44):

$$\begin{aligned}\mathcal{L}_{\rm tot} = {} & \frac{1}{4}\,\mathrm{Tr}\,\left[D_\mu\Sigma D^\mu\Sigma^\dagger\right] - \frac{\lambda}{8}\,\mathrm{Tr}\,\left[\left(\Sigma\Sigma^\dagger - f_0^2\right)^2\right] \\ & -\frac{\mu_\pi^2}{4}\,\mathrm{Tr}\,\left[(\Sigma - f_0)(\Sigma^\dagger - f_0)\right] - \frac{1}{4}\,\mathrm{Tr}\,\left[l_{\mu\nu}^2 + r_{\mu\nu}^2\right] + \frac{1}{2}\,m_0^2\,\mathrm{Tr}\,\left[l_\mu^2 + r_\mu^2\right] \\ & +\frac{1}{4}\,bg^2\,\mathrm{Tr}\,\left[\Sigma\Sigma^\dagger\right]\,\mathrm{Tr}\,\left[l_\mu^2 + r_\mu^2\right] - cg^2\,\mathrm{Tr}\,\left[l_\mu\Sigma r^\mu\Sigma^\dagger\right] - i\frac{\kappa_6 g}{4m_\rho^2} \\ & \times\mathrm{Tr}\,\left[l_{\mu\nu}D^\mu\Sigma D^\nu\Sigma^\dagger + r_{\mu\nu}D^{\mu\dagger}D^\nu\Sigma\right] - \frac{\zeta_6}{2m_\rho^2}\,\mathrm{Tr}\,\left[l_{\mu\nu}\Sigma r^{\mu\nu}\Sigma^\dagger\right], \end{aligned} \tag{A1}$$

where

$$\begin{aligned}\Sigma &= \sigma + i\boldsymbol{\tau}\cdot\boldsymbol{\pi}, \\ l_\mu &= (\boldsymbol{\rho}_\mu + \mathbf{a}_\mu)\cdot\mathbf{t}, \\ r_\mu &= (\boldsymbol{\rho}_\mu - \mathbf{a}_\mu)\cdot\mathbf{t},\end{aligned}$$

and $\mathbf{t}$'s are the generators of the SU(2) algebra. Working out the traces, one can write the above Lagrangian in terms of component fields:

$$\begin{aligned}\mathcal{L}_{\rm tot} = {} & \frac{1}{2}\left[(\Delta_\mu\sigma)^2 + (\Delta_\mu\boldsymbol{\pi})^2\right] - \frac{\lambda}{4}\left[\sigma^2 + \boldsymbol{\pi}^2 - f_0^2\right]^2 - \frac{\mu_\pi^2}{2}\left[\boldsymbol{\pi}^2 + (\sigma - f_0)^2\right] \\ & -\frac{1}{4}\left[\boldsymbol{\rho}_{\mu\nu} + g\left(\boldsymbol{\rho}_\mu\times\boldsymbol{\rho}_\nu + \mathbf{a}_\mu\times\mathbf{a}_\nu\right)\right]^2 - \frac{1}{4}\left[D_\mu\mathbf{a}_\nu - D_\nu\mathbf{a}_\mu\right]^2 + \frac{1}{2}\left[m_0^2 + bg^2(\sigma^2+\boldsymbol{\pi}^2)\right]\left(\boldsymbol{\rho}_\mu^2 + \mathbf{a}_\mu^2\right) \\ & +\frac{1}{2}\,cg^2\left[\sigma^2(\mathbf{a}_\mu^2 - \boldsymbol{\rho}_\mu^2) + 4\sigma\boldsymbol{\pi}\cdot(\boldsymbol{\rho}_\mu\times\mathbf{a}^\mu) - (\boldsymbol{\rho}_\mu\cdot\boldsymbol{\pi})^2 + (\mathbf{a}_\mu\cdot\boldsymbol{\pi})^2 - (\mathbf{a}_\mu\times\boldsymbol{\pi})^2 + (\boldsymbol{\rho}_\mu\times\boldsymbol{\pi})^2\right] \\ & +\frac{\kappa_6 g}{m_\rho^2}\left[(D_\mu\mathbf{a}_\nu - D_\nu\mathbf{a}_\mu)\cdot\Delta^\mu\boldsymbol{\pi}\Delta^\nu\sigma + \tfrac{1}{2}(\partial_\mu\boldsymbol{\rho}_\nu - \partial_\nu\boldsymbol{\rho}_\mu + g\boldsymbol{\rho}_\mu\times\boldsymbol{\rho}_\nu + g\mathbf{a}_\mu\times\mathbf{a}_\nu)\cdot\Delta^\mu\boldsymbol{\pi}\times\Delta^\nu\boldsymbol{\pi}\right] \\ & -\frac{\zeta_6}{4m_\rho^2}\left\{\left[\sigma^2(\boldsymbol{\rho}_{\mu\nu} + g\boldsymbol{\rho}_\mu\times\boldsymbol{\rho}_\nu + g\mathbf{a}_\mu\times\mathbf{a}_\nu)^2 - \sigma^2(D_\mu\mathbf{a}_\nu - D_\nu\mathbf{a}_\mu)^2 + 4\sigma\boldsymbol{\pi}\cdot(\boldsymbol{\rho}_{\mu\nu} + g\boldsymbol{\rho}_\mu\times\boldsymbol{\rho}_\nu + g\mathbf{a}_\mu\times\mathbf{a}_\nu)\right.\right. \\ & \times(D_\mu\mathbf{a}_\nu - D_\nu\mathbf{a}_\mu) + 2\left[(\boldsymbol{\rho}_{\mu\nu} + g\boldsymbol{\rho}_\mu\times\boldsymbol{\rho}_\nu + g\mathbf{a}_\mu\times\mathbf{a}_\nu)\cdot\boldsymbol{\pi}\right]^2 - 2\left\{(D_\mu\mathbf{a}_\nu - D_\nu\mathbf{a}_\mu)\cdot\boldsymbol{\pi}\right\}^2 \\ & \left.\left.-\boldsymbol{\pi}^2\left[(\boldsymbol{\rho}_{\mu\nu} + g\boldsymbol{\rho}_\mu\times\boldsymbol{\rho}_\nu + g\mathbf{a}_\mu\times\mathbf{a}_\nu)^2 - (D_\mu\mathbf{a}_\nu - D_\nu\mathbf{a}_\mu)^2\right]\right\}, \end{aligned} \tag{A2}$$

where

$$\begin{aligned}\Delta_\mu\sigma &= \partial_\mu\sigma + g\mathbf{a}_\mu\cdot\boldsymbol{\pi} \\ \Delta_\mu\boldsymbol{\pi} &= D_\mu\boldsymbol{\pi} - g\sigma\mathbf{a}_\mu \\ &= \partial_\mu\boldsymbol{\pi} + g\boldsymbol{\rho}_\mu\times\boldsymbol{\pi} - g\sigma\mathbf{a}_\mu, \\ D_\mu\mathbf{a}_\nu &= \partial_\mu\mathbf{a}_\nu + g\boldsymbol{\rho}_\mu\times\mathbf{a}_\nu.\end{aligned} \tag{A3}$$

After the σ field acquires a vacuum expectation value $\langle\sigma\rangle = f_0$, one makes the shifts

$$\sigma \to \sigma + f_0,$$

$$\mathbf{a}_\mu \to \mathbf{a}_\mu + hD_\mu\boldsymbol{\pi}.$$

The quadratic pieces of the resulting Lagrangian are given as

$$\begin{aligned}\mathcal{L}_{\rm kin} = &\frac{1}{2}\left[(\partial_\mu\sigma)^2 + Z_\pi\,(D_\mu\boldsymbol{\pi})^2\right] - \frac{Z_\rho}{4}\,\boldsymbol{\rho}_{\mu\nu}^2 \\ &+\frac{1}{2}\,\boldsymbol{\rho}_\mu^2\,\left[m_0^2 + (b-c)g^2f_0^2\right] \\ &-\frac{Z_a}{4}\,(D_\mu\mathbf{a}_\nu - D_\nu\mathbf{a}_\mu)^2 \\ &+\frac{1}{2}\,\mathbf{a}_\mu^2\,\left[m_0^2 + (b+c+1)g^2f_0^2\right] + \mathbf{a}_\mu\cdot D^\mu\boldsymbol{\pi} \\ &\times\{-gf_0\,(1-gf_0h) + \left[m_0^2 + (b+c)g^2f_0^2\right]h\},\end{aligned} \tag{A4}$$

where

$$Z_\pi = (1-ghf_0)^2 + \left[m_0^2 + (b+c)g^2f_0^2\right]h^2, \tag{A5}$$

$$Z_\rho = 1 + \frac{\zeta_6 f_0^2}{m_\rho^2}, \tag{A6}$$

$$Z_a = 1 - \frac{\zeta_6 f_0^2}{m_\rho^2}. \tag{A7}$$

By rescaling the fields $\boldsymbol{\pi}, \boldsymbol{\rho}$, and $\mathbf{a}$ to get the canonical forms of kinetic energy terms, we get

$$m_\rho^2 = \frac{1}{Z_\rho}\,\left[m_0^2 + (b-c)g^2f_0^2\right], \tag{A8}$$

$$m_{a_1}^2 = \frac{1}{Z_a}\,\left[m_0^2 + (b+c+1)g^2f_0^2\right]. \tag{A9}$$

Removing the $a_1 - \pi$ mixing term, we get

$$h = \frac{gf_0}{Z_a m_{a_1}^2}, \tag{A10}$$

and, hence,

$$\begin{aligned}Z_\pi &= 1 - ghf_0 = 1 - \frac{g^2f_0^2}{Z_a m_{a_1}^2} \\ &= 1 - \left(\frac{1}{2c+1}\right)\left(1 - \frac{Z_\rho m_\rho^2}{Z_a m_{a_1}^2}\right).\end{aligned} \tag{A11}$$

First of all, the $\rho\pi\pi$ coupling is described by ($\boldsymbol{\pi} \equiv \boldsymbol{\pi}_r/\sqrt{Z_\pi}$ and similarly for $\boldsymbol{\rho}$ and $\mathbf{a}$ fields)

$$\begin{aligned}\mathcal{L}(\rho\pi\pi)\times Z_\pi\sqrt{Z_\rho} = &-\frac{gZ_\rho m_\rho^2}{Z_a m_{a_1}^2}\,\boldsymbol{\rho}_{r,\mu}\cdot(\partial^\mu\boldsymbol{\pi}_r\times\boldsymbol{\pi}_r) \\ &-\frac{g}{2}\left[h^2Z_\rho + \frac{Z_\pi^2\kappa_6}{m_\rho^2}\right] \\ &\times\boldsymbol{\rho}_{r,\mu\nu}\cdot(\partial^\mu\boldsymbol{\pi}_r\times\partial^\nu\boldsymbol{\pi}_r),\end{aligned} \tag{A12}$$

from which we get the momentum-dependent form factor $F_{\rho\pi\pi}(q^2)$ given in Eq. (2.29). This also contributes to Eq. (3.11) in the $\pi\pi$ scattering.

The π^4 interaction is described by

$$\mathcal{L}(\pi^4) = -\frac{\lambda}{4Z_\pi^2}\,\boldsymbol{\pi}_r^4 + \frac{g^2h^2}{2Z_\pi^2}\,\{(\boldsymbol{\pi}_r\cdot\partial_\mu\boldsymbol{\pi}_r)^2 + b\,\boldsymbol{\pi}_r^2\,(\partial_\mu\boldsymbol{\pi}_r)^2 + c[(\boldsymbol{\pi}_r\cdot\partial_\mu\boldsymbol{\pi}_r)^2 - (\partial_\mu\boldsymbol{\pi}_r\times\boldsymbol{\pi}_r)^2]\}, \tag{A13}$$

where the second term is induced via π-a_1 mixing. This contributes to Eq. (3.9) in the $\pi\pi$ scattering. Note that the κ_6 term does not contribute to the π^4 vertex.

The $\sigma\pi\pi$ coupling is described by

$$\mathcal{L}(\sigma\pi\pi) = -\frac{\lambda f_0}{Z_\pi}\,\sigma\boldsymbol{\pi}_r^2 - \frac{gh}{Z_\pi}\,\left[\sigma\boldsymbol{\pi}_r\cdot\partial^2\boldsymbol{\pi}_r + \left(1 + \frac{m_0^2}{Z_a m_{a_1}^2}\right)\,\sigma(\partial_\mu\boldsymbol{\pi}_r)^2\right]. \tag{A14}$$

The second line is induced via $\pi - a_1$ mixing, and affects the $\pi\pi$ scattering [Eq. (3.10)] and the width of σ [Eq. (3.13)]. Note that the κ_6 term does not contribute to the $\sigma\pi\pi$ coupling.

The $a_1\rho\pi$ coupling is described by

$$\begin{aligned}\mathcal{L}(a_1\rho\pi) = \frac{g^2f_\pi}{Z_\pi\sqrt{Z_\rho Z_a}}\,&\left[2c\,\boldsymbol{\pi}_r\cdot(\boldsymbol{\rho}_{r,\mu}\times\mathbf{a}_r^\mu) + \frac{1}{m_\rho^2}\left(\frac{m_\rho^2}{2m_{a_1}^2} - \frac{\zeta_6}{g^2}\right)\,\boldsymbol{\pi}_r\cdot\boldsymbol{\rho}_{r,\mu\nu}\times\mathbf{a}_r^{\mu\nu}\right. \\ &\left.+\frac{1}{m_\rho^2}\left(\frac{Z_\rho m_\rho^2}{Z_a m_{a_1}^2} - \kappa_6 Z_\pi\right)\,\partial_\mu\boldsymbol{\pi}_r\cdot\boldsymbol{\rho}_r^{\mu\nu}\times\mathbf{a}_{r,\nu}\right].\end{aligned} \tag{A15}$$

This interaction Lagrangian gives two form factors for $a_1 \to \rho\pi$, Eqs. (4.2) and (4.3) for $\zeta_6 = 0$. Note that $g_{a_1\rho\pi} = 0$ if $\kappa_6 = 0$.

The $a_1\sigma\pi$ vertex is given by

$$\mathcal{L}(a_1\sigma\pi) = -\frac{g}{\sqrt{Z_\pi Z_a}}\,\left[\frac{2m_0^2}{Z_a m_{a_1}^2} - \kappa_6 Z_\pi\,\frac{m_{a_1}^2}{m_\rho^2}\right]\,\mathbf{a}_{r,\mu}\cdot\partial^\mu\boldsymbol{\pi}_r\sigma. \tag{A16}$$

We note that the amplitude for $a_1 \to \sigma\pi$ vanishes, if $m_0 = \kappa_6 = 0$.

The $a_1 3\pi$ coupling is determined from

$$\mathcal{L}(a_1\pi^3)\times\sqrt{Z_{a_1}Z_\pi^3}=\frac{1}{2}\,g^2h(2b-c-1)\,\mathbf{a}_{r,\mu}\cdot\partial^\mu\boldsymbol{\pi}_r\,\boldsymbol{\pi}_r^2-cg^2h\mathbf{a}_{r,\mu}\times\boldsymbol{\pi}_r\cdot\partial_\mu\boldsymbol{\pi}_r\times\boldsymbol{\pi}_r-\frac{\kappa_6 g^2hZ_\pi}{m_\rho^2}$$
$$\times\left[\mathbf{a}_{r,\mu\nu}\cdot\partial_\mu\boldsymbol{\pi}_r\,\boldsymbol{\pi}_r\cdot\partial_\nu\boldsymbol{\pi}_r+Z_\pi\left(1-\frac{gf_0h}{Z_\pi}\right)\,\mathbf{a}_{r,\mu}\times\partial_\nu\boldsymbol{\pi}_r\cdot\partial_\mu\boldsymbol{\pi}_r\times\partial_\nu\boldsymbol{\pi}_r\right]. \tag{A17}$$

The corresponding vertex for the usual nonlinear σ model can be obtained from (A17) by setting $b=0$.

Finally, we present the vector and the axial vector currents in the presence of dimension-6 operators:

$$\mathbf{V}_\mu=\frac{m_\rho^2\sqrt{Z_\rho}}{g}\,\boldsymbol{\rho}_{r,\mu}-\frac{2cgf_0h}{Z_\pi\sqrt{Z_a}}\,\boldsymbol{\pi}_r\times\partial_\mu\boldsymbol{\pi}_r-\frac{2cgf_0\boldsymbol{\pi}_r\times\mathbf{a}_{r,\mu}}{\sqrt{Z_\pi\,Z_a}}+\cdots, \tag{A18}$$

$$\mathbf{A}_\mu=\frac{m_{a_1}^2Z_\pi\sqrt{Z_a}}{g}\,\mathbf{a}_{r,\mu}+f_0\sqrt{Z_\pi}\,D_\mu\boldsymbol{\pi}_r+\cdots. \tag{A19}$$

For $Z_a=Z_\rho=1$, we recover the expressions given in (2.14) and (2.15). From (A18), we can infer that the data on $\rho^0\to e^+e^-$ actually constraint $g/\sqrt{Z_\rho}$ to be 5.04.

APPENDIX B: NON-$\rho\pi$ CONTRIBUTIONS TO $A_1\to 3\pi$

In this section, we give explicit expressions for the form factors defined in (4.15). The relevant Feynman diagrams are shown in Figs. 7(a) and 7(b). To get the non$-\rho\pi$ contributions to $a_1^+\to(3\pi)^+$, we ignore the $\rho\pi$ contribution. We need to consider two distinct final states:

$$a_1(k,\epsilon)\to\pi^+(p_1)\pi^+(p_2)\pi^-(p_3),$$
$$\to\pi^0(p_1)\pi^0(p_2)\pi^+(p_3).$$

Evaluating Figs. 7(a) and 7(b), we get

$$G_1^{(a)}(++-)=\frac{G_{a_1\sigma\pi}\,G_{\sigma\pi\pi}(s_{13})}{s_{13}-m_\sigma^2+i\sqrt{s_{13}}\Gamma_\sigma(s_{13})}, \tag{B1}$$

$$G_2^{(a)}(++-)=-G_{a_1\sigma\pi}\left[\frac{G_{\sigma\pi\pi}(s_{23})}{s_{23}-m_\sigma^2+i\sqrt{s_{23}}\Gamma_\sigma(s_{23})}-\frac{G_{\sigma\pi\pi}(s_{13})}{s_{13}-m_\sigma^2+i\sqrt{s_{13}}\Gamma_\sigma(s_{13})}\right], \tag{B2}$$

$$G_1^{(a)}(00+)=-\frac{G_{a_1\sigma\pi}\,G_{\sigma\pi\pi}(s_{12})}{s_{12}-m_\sigma^2+i\sqrt{s_{12}}\Gamma_\sigma(s_{12})}, \tag{B3}$$

$$G_2^{(a)}(00+)=0, \tag{B4}$$

$$G_1^{(b)}(++-)=-\frac{i}{\sqrt{Z_\pi^3}}\left\{g^2h(2b-4c-1)+\kappa_6g^2hZ_\pi\frac{m_{a_1}^2}{m_\rho^2}+\left[\frac{1}{2}g^2h^3+\frac{\kappa_6g^2hZ_\pi^2}{m_\rho^2}\left(1-\frac{ghf_0}{Z_\pi}\right)\right](2p_1\cdot p_2+p_1\cdot p_3)\right\}, \tag{B5}$$

$$G_2^{(b)}(++-)=\frac{i}{\sqrt{Z_\pi^3}}\left[\frac{1}{2}g^2h^3+\frac{\kappa_6g^2hZ_\pi^2}{m_\rho^2}\left(1-\frac{ghf_0}{Z_\pi}\right)\right](p_2-p_1)\cdot p_3, \tag{B6}$$

$$G_1^{(b)}(00+)=-G_1^{(b)}(++-), \tag{B7}$$

$$G_1^{(b)}(00+)=-G_1^{(b)}(++-). \tag{B8}$$

Here, $G_{a_1\sigma\pi}$ and $G_{\sigma\pi\pi}(s)$ are defined in (4.12) and (3.13), and $s_{ij}\equiv(p_i+p_j)^2$.

The non$-\rho\pi$ contributions to the decay $a_1\to(3\pi)^+$ can be obtained by integrating the following expression over $s\equiv s_{12}$ and $t\equiv s_{13}$:

$$\frac{d^2\Gamma}{dsdt}=\frac{1}{2(2\pi)^3}\,\frac{1}{32m_{a_1}^2}\,\frac{1}{3}\left\{|G_1^{\rm tot}|^2|\mathbf{p}_3|^2+|G_2^{\rm tot}|^2\left[\frac{(k\cdot p_1)^2}{m_{a_1}^2}-m_\pi^2\right]+\left(G_1^{\rm tot}G_2^{tot*}+G_1^{tot*}G_2^{\rm tot}\right)\left[\frac{k\cdot p_1\;k\cdot p_3}{m_{a_1}^2}-p_1\cdot p_3\right]\right\}, \tag{B9}$$

where

$$G_{1,2}^{\rm tot}(++-)=G_{1,2}^{(a)}(++-)+G_{1,2}^{(b)}(++-),$$
$$G_{1,2}^{\rm tot}(00+)=G_{1,2}^{(a)}(00+)+G_{1,2}^{(b)}(00+).$$

The integration limits for s, t are given by

$$4m_\pi^2 \leq s \leq (m_{a_1} - m_\pi)^2,$$
$$t_{\min} \leq t \leq t_{\max},$$

with

$$E_1^* = \tfrac{1}{2}\sqrt{s_{12}},$$
$$E_3^* = \frac{m_{a_1}^2 - s_{12} - m_\pi^2}{2\sqrt{s_{12}}},$$
$$t_{\min,\max} = (E_1^* + E_3^*)^2 - \left[\sqrt{E_1^{*2} - m_\pi^2} \pm \sqrt{E_3^{*2} - m_\pi^2}\right]^2.$$

Finally, the above expression must be summed over distinct final states.

[1] Particle Data Group, L. Montanet *et al.*, Phys. Rev. **D 50**, 1173 (1994).
[2] D. Morgan and M.R. Pennington, Phys. Rev. D **48**, 1185 (1993).
[3] M. Gell-Mann and M. Levy, Nuovo Cimento **16**, 705 (1960).
[4] J. Schwinger, Phys. Lett. **24B**, 473 (1967); J. Wess and B. Zumino, Phys. Rev. **163**, 1727 (1967); B.W. Lee and H.T. Nieh, *ibid.* **166**, 1507 (1968).
[5] S. Gasiorowicz and D. Geffen, Rev. Mod. Phys. **41**, 531 (1969); S. Gasiorowicz, Acta Phys. Austriaca, Suppl. VI, 19 (1969).
[6] J. Boguta, Phys. Lett. **120B**, 34 (1983); see also E.K. Heide, P.J. Ellis, and S. Rudaz, Phys. Lett. B **293**, 259 (1992); Nucl. Phys. **A571**, 713 (1994).
[7] Ö. Kaymakcalan and J. Schechter, Phys. Rev. D **31**, 1109 (1985).
[8] K. Kawarabayashi and M. Suzuki, Phys. Rev. Lett. **16**, 255 (1966); Fayyazuddin and Riazuddin, Phys. Rev. **147**, 1071 (1966).
[9] H.J. Schnitzer and S. Weinberg, Phys. Rev. **164**, 1828 (1967).
[10] J. Gasser and H. Leutwyler, Ann. Phys. (N.Y.) **158**, 142 (1984).
[11] Ulf.-G. Meissner, Phys. Rep. **161**, 213 (1988).
[12] N. Kroll, T.D. Lee, and B. Zumino, Phys. Rev. **157**, 1376 (1967).
[13] J. Gasser and Ulf.-G. Meissner, Phys. Lett. B **258**, 219 (1991); V. Bernard, N. Kaiser, and Ulf.-G. Meissner, Nucl. Phys. **B364**, 283 (1991).
[14] D. Geffen, Phys. Rev. Lett. **19**, 770 (1967); S.G. Brown and G.B. West, *ibid.* **19**, 812 (1967).
[15] N. Isgur, C. Morningstar, and C. Reader, Phys. Rev. D **39**, 1357 (1989).
[16] H. Albrecht *et al.*, Z. Phys. **C 58**, 61 (1993).
[17] M. Zielinski *et al.*, Phys. Rev. Lett. **52**, 1195 (1984).
[18] Fayyazuddin and Riazuddin, Phys. Rev. Lett. **18**, 715 (1967).
[19] J.L. Rosner, Phys. Rev. D **23**, 1127 (1981).
[20] L. Xiong, E. Shuryak, and G.E. Brown, Phys. Rev. D **46**, 3798 (1992).
[21] M. Bando, T. Kugo, and K. Yamawaki, Nucl. Phys. **B259**, 493 (1986); M. Bando, T. Fujiwara, and K. Yamawaki, Prog. Theor. Phys. **79**, 1140 (1988).
[22] I. Gerstein and H.J. Schnitzer, Phys. Rev. **175**, 1638 (1968).
[23] E. Witten, Nucl. Phys. **B223**, 422 (1983); Ö. Kaymakcalan, S. Rajeev, and J. Schechter, Phys. Rev. D **30**, 594 (1984); T. Fujiwara, T. Kugo, H. Terao, S. Uehara, and K. Yamawaki, Prog. Theor. Phys. **73**, 926 (1985).
[24] M. Gell-Mann, D. Sharp, and W.G. Wagner, Phys. Rev. Lett. **8**, 261 (1962).